Journal of Medicinal Chemistry

Article

pubs.acs.org/jmc

Novel N-Linked Aminopiperidine-Based Gyrase Inhibitors with Improved hERG and in Vivo Efficacy against *Mycobacterium tuberculosis*

Shahul Hameed P,*[,†] Vikas Patil,[†] Suresh Solapure,[§] Umender Sharma,[‡] Prashanti Madhavapeddi,[‡] Anandkumar Raichurkar,[†] Murugan Chinnapattu,[†] Praveena Manjrekar,[†] Gajanan Shanbhag,[†] Jayashree Puttur,[†] Vikas Shinde,[†] Sreenivasaiah Menasinakai,[†] Suresh Rudrapatana,[†] Vijayashree Achar,[†] Disha Awasthy,[‡] Radha Nandishaiah,[‡] Vaishali Humnabadkar,[‡] Anirban Ghosh,[‡] Chandan Narayan,[‡] V. K. Ramya,[‡] Parvinder Kaur,[‡] Sreevalli Sharma,[‡] Jim Werngren,[#] Sven Hoffner,[#] Vijender Panduga,[§] C. N. Naveen Kumar,[§] Jitendar Reddy,[§] Mahesh Kumar KN,[§] Samit Ganguly,[§] Sowmya Bharath,[§] Ugarkar Bheemarao,[†] Kakoli Mukherjee,[‡] Uma Arora,[§] Sheshagiri Gaonkar,[§] Michelle Coulson,[∥] David Waterson,[⊥] Vasan K. Sambandamurthy,[‡] and Sunita M. de Sousa[‡]

[†]Department of Medicinal Chemistry; [‡]Department of Biosciences and [§]DMPK and Animal Sciences, AstraZeneca India Pvt. Ltd., Bellary Road, Hebbal, Bangalore 560024, India

[∥]Safety Assessment, AstraZeneca, Alderley Park, Macclesfield, U.K.

Supporting Information

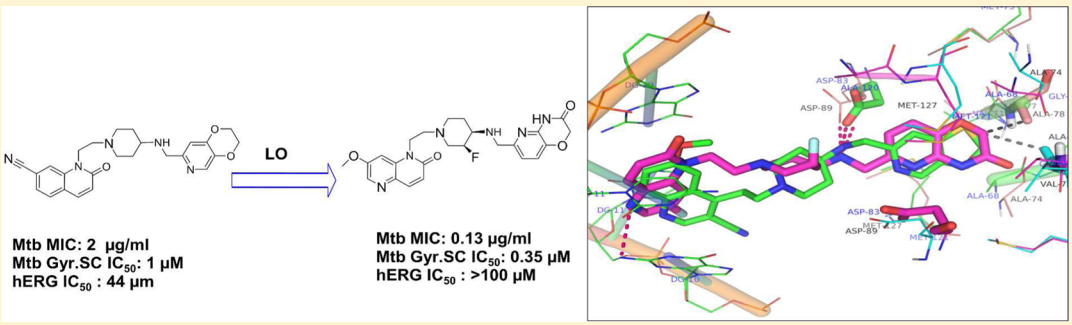

ABSTRACT: DNA gyrase is a clinically validated target for developing drugs against *Mycobacterium tuberculosis* (Mtb). Despite the promise of fluoroquinolones (FQs) as anti-tuberculosis drugs, the prevalence of pre-existing resistance to FQs is likely to restrict their clinical value. We describe a novel class of N-linked aminopiperidinyl alkyl quinolones and naphthyridones that kills Mtb by inhibiting the DNA gyrase activity. The mechanism of inhibition of DNA gyrase was distinct from the fluoroquinolones, as shown by their ability to inhibit the growth of fluoroquinolone-resistant Mtb. Biochemical studies demonstrated this class to exert its action via single-strand cleavage rather than double-strand cleavage, as seen with fluoroquinolones. The compounds are highly bactericidal against extracellular as well as intracellular Mtb. Lead optimization resulted in the identification of potent compounds with improved oral bioavailability and reduced cardiac ion channel liability. Compounds from this series are efficacious in various murine models of tuberculosis.

INTRODUCTION

Tuberculosis (TB) continues to be a major global health problem that claims ∼1.5 million lives each year and imposes a huge economic burden on developing countries.[1] This problem is further aggravated by the emergence of drug-resistant strains of Mtb that require up to 2 years of treatment with a combination of six to eight drugs.[2]

The availability of the genome sequence of Mtb has propelled a huge effort toward target-based discovery of antimycobacterial compounds.[3] However, numerous efforts aimed at the essential targets in Mtb have highlighted many inherent challenges in identifying attractive chemical leads.[4] Clinically validated targets of known antimycobacterial agents offer a great promise in terms of designing novel inhibitors that are likely to be bactericidal under the in vitro and in vivo growth conditions. Among the extensively studied bacterial targets, DNA gyrase, belonging to the type II topoisomerase family, has been validated clinically by the fluoroquinolone (FQ) class of drugs.[5a,b] Combination regimens containing moxifloxacin have shown the potential to shorten the duration of TB treatment.[5c] However, pre-existing resistance to FQs is

Received: March 19, 2014

   dx.doi.org/10.1021/jm500432n | J. Med. Chem. XXXX, XXX, XXX−XXX

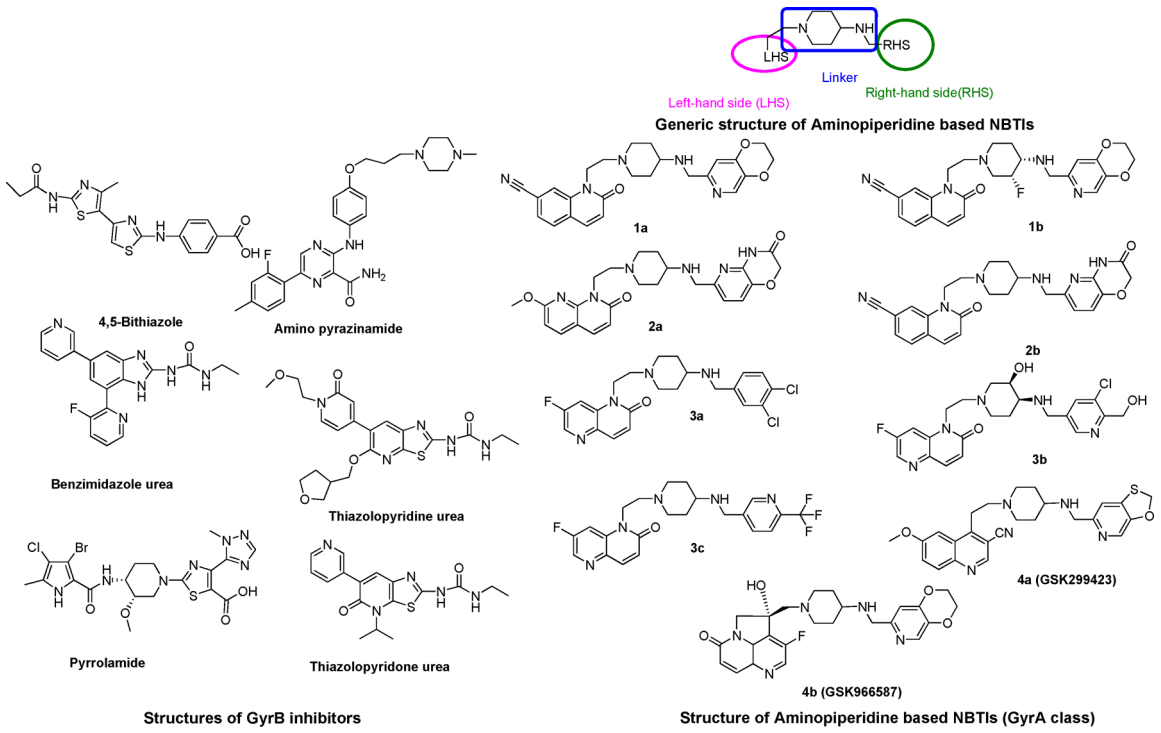

Figure 1. Non-fluoroquinolone-based gyrase inhibitors reported in the literature.

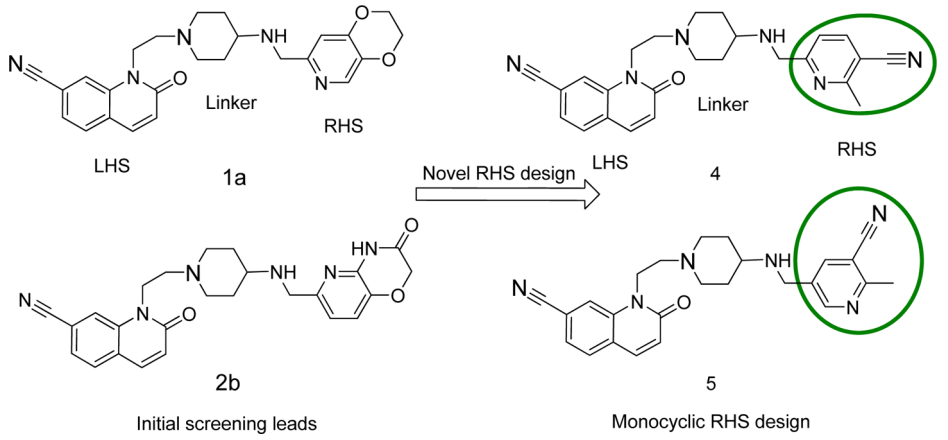

Figure 2. Structures of initial leads (**1a**, **2b**) and compounds with monocyclic RHS (**4**, **5**).

likely to limit the clinical utility of this class of drugs for treating TB in the long run.[5d]

FQs bind to the GyrA subunit of bacterial DNA gyrase and trap the double strand cleaved DNA–gyrase complex, inducing an SOS response that leads to bacterial cell death.[6] A novel inhibitor of the DNA gyrase with a unique binding site is likely to have activity against FQ-resistant TB. Numerous non-fluoroquinolone-based bacterial type II topoisomerase inhibitors from both the GyrA and GyrB classes have been reported as antibacterial agents.[7] Inhibitors of the DNA GyrB class include bisthiazoles,[18a] aminopyrazinamides,[18b] aryl ureas,[18c,e] and pyrrolamides,[18d] whereas inhibitors of the GyrA class include aminopiperidine-based novel bacterial type II topoisomerase inhibitors (NBTIs). AstraZeneca has reported novel N-linked aminopiperidines as potent inhibitors of the bacterial type II topoisomerases with antibacterial activity.[9−11] GlaxoSmithKline (GSK) has reported antibacterial and anti-TB activity for NBTIs with in vivo efficacy in the acute mouse model of TB.[12,13] Representative structures of the GyrA class, N-linked aminopiperidines (**1a**, **1b**, **2a**, and **2b**)[9−11] from AstraZeneca, and NBTIs (**3a**, **3b**, **3c**, **4a**, and **4b**)[12,13] from GSK are shown in Figure 1.

The chemical structures of NBTIs including the N-linked piperidines consist of three parts, namely, a bicyclic aromatic left-hand side (LHS), a mono or bicyclic right-hand side (RHS), and a linker region joining the RHS and LHS.

The mechanism of inhibition and the binding mode of NBTIs for the antibacterial series have been reported.[8a] From the crystal structure studies of methoxyquinoline-3-carbonitrile (GSK299423, **4a**),[8a] one can infer that the LHS portion of the NBTIs binds to the DNA substrate, whereas the RHS portion interacts with the protein dimer interface of the GyrA subunits. The binding site of NBTIs is distinct from the FQ binding, and they are reported to be active against FQ-resistant strains of *Staphylococcus aureus*.[8a] However, the mode of binding of NBTIs to the Mtb GyrA subunit is not known. As the active

dx.doi.org/10.1021/jm500432n | J. Med. Chem. XXXX, XXX, XXX−XXX

Scheme 1[a]

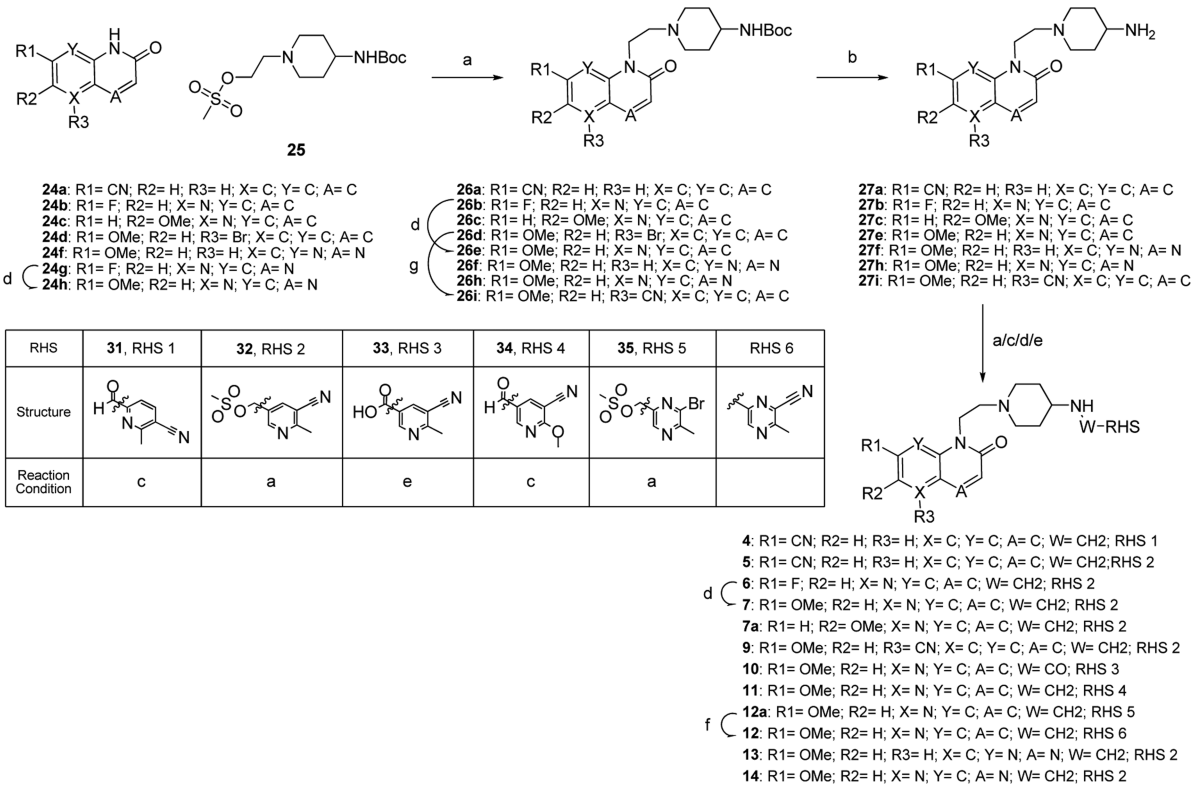

RHS	31, RHS 1	32, RHS 2	33, RHS 3	34, RHS 4	35, RHS 5	RHS 6
Structure						
Reaction Condition	c	a	e	c	a	

[a]Reagents: (a) Na_2CO_3, DMF, 70 °C; (b) 4 N HCl in dioxane, 55 °C; (c) $NaBH_3CN$, DCE or $CHCl_3$/EtOH, 65−80 °C; (d) NaOMe, MeOH, 75 °C; (e) **33**, HATU, DIPEA, DMF, rt; (f) $ZnCN_2$, $Zn(OAc)_2$, Zn, $Pd_2(dba)_3$, dppf, DMF, 100 °C, 23%; (g) $Pd_2(dba)_3$, dppf, CuCN, DMF, 110 °C, 68%.

Scheme 2[a]

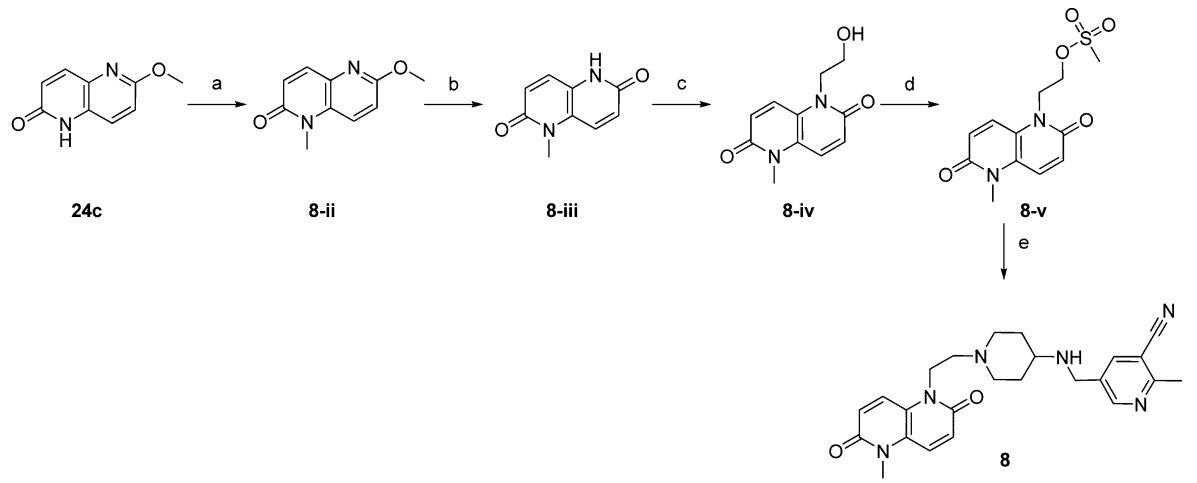

[a]Reagents: (a) MeI, Cs_2CO_3, DMSO, 60 °C, 83%; (b) 48% HBr, 80 °C, > 95%; (c) 2-bromoethanol, Cs_2CO_3, DMSO, 95 °C, >95%; (d) MsCl, TEA, DCM, 0 °C, >95%; (e) **29e**, Na_2CO_3, DMF, 70 °C, 98%.

site of DNA gyrases is highly conserved across the bacterial species, we assumed that the binding mode could be similar to what has been reported for *S. aureus* DNA gyrase.[8b]

The NBTIs with a monocyclic RHS (**3a**−**3c**) display potent minimum inhibitory concentration (MIC) against FQ-sensitive and FQ-resistant strains of Mtb and were found to be efficacious in the acute mouse model of tuberculosis.[13a] However, these compounds are also potent inhibitors of the cardiac hERG channel.[13b] A different class of N-linked aminopiperidines with a bicyclic RHS and an optimized linker was shown to have lesser hERG liability.[10,11] Therefore, we screened a library of N-linked aminopiperidines against Mtb and identified lead compounds that inhibited Mtb DNA gyrase activity as well as the growth of Mtb in broth (Figure2). Herein, we report medicinal chemistry efforts to reduce the hERG liability and improve the Mtb MIC as well as the oral bioavailability of these lead molecules. Additionally, we also describe the mechanism of inhibition of Mtb gyrase, the

dx.doi.org/10.1021/jm500432n | J. Med. Chem. XXXX, XXX, XXX−XXX

Scheme 3[a]

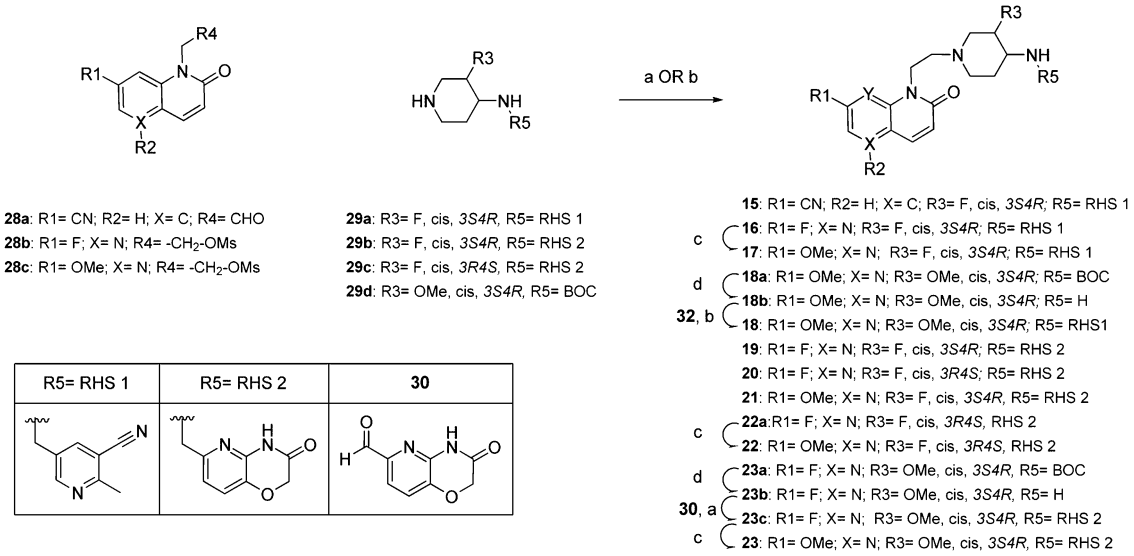

[a]Reagents: for R4 = CHO, (a) $NaBH(OAc)_3$, DMF, 70 °C; for R4 = $-CH_2-OMs$, (b) Na_2CO_3, DMF, 70 °C; (c) NaOMe, MeOH, 75 °C; (d) 4 N HCl in dioxane, 55 °C or TFA/DCM, rt.

Table 1. Properties of the Initial Lead Compounds (1a, 2a, 2b) and the Novel Compounds with a Monocyclic RHS (4 and 5)

properties	1a	2a	2b	4	5
Mtb MIC (μg/mL)	2	0.25	0.13	>16	0. 06
Mtb gyrase supercoiling IC_{50} (μM)	1.05	0.150	0.110	>100	0.25
Msm GyrB ATPase IC_{50} (μM)	>100	>100	>100	>100	>100
log *D* pH 7.4	0.7	0.8	0.4	1.1	1.3
hERG IC_{50} (μM)	44	21	ND	5.3	26
Caco-2: Papp A–B/B–A (1×10^{-6} cm/s)	1.9/38.3	1.1/25	2.0/12.6	17.1/9.1	13.6/7.4

characterization of spontaneous resistant mutants, and the efficacy in the acute and chronic mouse model of TB.

CHEMISTRY

The synthesis of compounds with unsubstituted aminopiperidine and methoxy- or fluoro-substituted aminopiperidine linker is described in Schemes 1,2, and 3, respectively. The alkylation of the LHS (**24a–h**) with mesylate **25** in the presence of a base resulted in the formation of *N*-alkylated product (**26a–i**) as the major isomer along with a small amount of *O*-alkylated product. Wherever possible, the minor *O*-alkylated isomer was removed by column chromatography;[11] otherwise, the mixture was taken as such for *N*-Boc deprotection. The free amines (**27a–i**) were obtained upon *N*-Boc deprotection of the intermediates **26a–i** in the presence of an acid. Compounds **4–14** were synthesized from the amines **27a–i** either by reductive amination with RHS aldehydes (**31**, **34**), by amide coupling with RHS acid (**33**), or by alkylation with mesylates (**32**, **35**) (Scheme 1). The mesylate **25** and LHS fragments **24a** and **24f** were synthesized as reported by Reck et al.,[10,11] whereas LHS fragments **24b** and **24c** were synthesized using an optimized Heck protocol as described earlier.[14] The synthesis of **24d** as described in Scheme 6 (Supporting Information). The LHS **24h** was synthesized from its fluoro precursor **24g** using NaOMe.[15] Detailed synthesis of the precursor aldehydes **31** and **34**, the mesylates **32** and **35**, and acid **33** are described in Schemes 7 and 8 (Supporting Information).

Compound **8** was synthesized as described in Scheme 2. The intermediate naphthyridone **24c** was *N*-methylated with methyl iodide in the presence of cesium carbonate to generate intermediate **8-ii**. *O*-Demethylation of **8-ii** with HBr provided the naphthyridine-2,6-dione **8-iii**, which upon alkylation with 2-bromoethanol gave both the *N*- and *O*-alkylated isomers. The *N*-alkylated isomer **8-iv** was converted to mesylate **8-v** with MsCl under basic conditions. The alkylation of **29e** with mesylate **8-v** under basic conditions resulted in compound **8**.

The synthesis of compounds with substituted aminopiperidine linker is shown in Scheme 3. The RHS aldehyde **30** was synthesized as reported earlier.[16] The reductive amination of the modified aminopiperidine linkers (**29a–d**) with the LHS aldehyde (**28a**) or alkylation with mesylates (**28b,c**) in the presence of a base provided the final compounds (**15–17**, **19–21**) in moderate to good yields. The compounds **18** and **23** were obtained by alkylation of **18b** with mesylate **32** and reductive amination of **23b** with aldehyde **30**, respectively. Synthesis of all the intermediates involved in Schemes 1–3 are described in the Supporting Information.

RESULTS AND DISCUSSION

Identification of Lead Molecules. A focused library of N-linked aminopiperidines, synthesized during the antibacterial drug discovery program, was screened for MIC against replicating Mtb in broth. This screening effort led to the identification of compounds **1a**, **2a**, and **2b** with submicromolar MIC against Mtb. Properties of the representative lead molecules are shown in Table 1.

dx.doi.org/10.1021/jm500432n | J. Med. Chem. XXXX, XXX, XXX–XXX

As shown in Table 1, the compounds **1a**, **2a**, and **2b** displayed low micromolar or submicromolar Mtb MIC along with potent IC_{50} in the Mtb DNA gyrase supercoiling (SC) assay. The specific activity of the Mtb enzyme was too low to set up a specific assay for ATPase activity of Mtb set up a specific assay for ATPase activity of Mtb GyrB.[18b] Therefore, we have used *Mycobacterium smegmatis* (Msm) GyrB as a surrogate for the Mtb enzyme.[18b] None of the initial leads inhibited the ATPase activity of Msm GyrB, suggesting that the holoenzyme (GyrA2B2 complex) or GyrA was inhibited. Initial leads inhibited the hERG channel and had poor Caco2 permeability. Lead optimization efforts were primarily focused on improving the Mtb MIC and Caco2 permeability and reducing the hERG liability. During lead optimization, we tracked the SAR based on Mtb MIC assuming that the mechanism of gyrase inhibition was retained across newly synthesized compounds in this series.

Lead Optimization and Hypothesis Generation. We hypothesized that reducing the number of hydrogen-bonding groups while keeping log *D* in the range of 1−2 would improve the Caco-2 permeability and maintain MIC. Compounds **4** and **5** having disubstituted pyridines with hydrophilic and electron-withdrawing cyano substitution were designed by opening the bicyclic RHS ring. A shape-based overlay of the newly designed analogues (**4** and **5**) with the initial leads (**1a** and **2a** in Figure 2) using the ROCS[19] tool suggested that the overall shape of molecules on the LHS or the linker region was similar (Figure 3).

The RHS fragment with the 3-pyridyl ring in compound **5** fully occupies the shape of the bicyclic RHS (**1a** and **2b**), thereby suggesting that their binding mechanism could be similar. In the case of compound **4**, the RHS with 2-pyridyl ring did not fully occupy the shape of the bicyclic RHS ring (**1a** and **2b**) of the initial leads. Hence, compound **4** may have different behavior with respect to the enzyme potency. On the basis of this hypothesis, compounds **4** and **5** were synthesized and tested. Compound **5** maintained good enzyme potency and MIC, whereas as compound **4** lost both of these activities.

Due to the nonavailability of a cocrystal structure of Mtb gyrase, we docked compounds **4** and **5** into the published crystal structure of *S. aureus* DNA bound GyrA subunit (PDB ID 2XCS).[8a] Subsequently, a Mtb DNA gyrase subunit A (Mtb GyrA) homology model was built on 2XCS as a template using MOE.[20] FRED[21] docking tool was used understand the binding interactions. Parts b,c and d of Figure 3 show the possible binding modes of compounds **4** and **5** in the DNA-bound GyrA subunit of *S. aureus* and in the Mtb GyrA model, respectively. Docking analysis suggested that the LHS quinolone of compounds **4** and **5** were positioned between the two base pairs of DNA, as observed for NBTIs, whereas the RHS pyridine binding showed a subtle difference with respect to the methyl group orientation. The methyl substitution in the RHS of compound **5** was oriented toward the hydrophobic region occupied by Ala68, Val71, Gly72, and Met121 of the DNA-bound GyrA subunit of *S. aureus* (Ala74, Val77, Ala78, and Met127 in the Mtb GyrA, respectively) making several van der Waals contacts. The methyl group also makes a stronger interaction with the carbonyl of Ala74 and methyl of Ala78 in Mtb. On the contrary, the methyl group of the RHS pyridine in compound **4** was oriented away from the hydrophobic region (Figure 3d) and the nitrile group was in close proximity to Ala 74. Additionally, the −NH group of the aminopiperidine ring in compound **5** makes a key interaction with the carboxylate

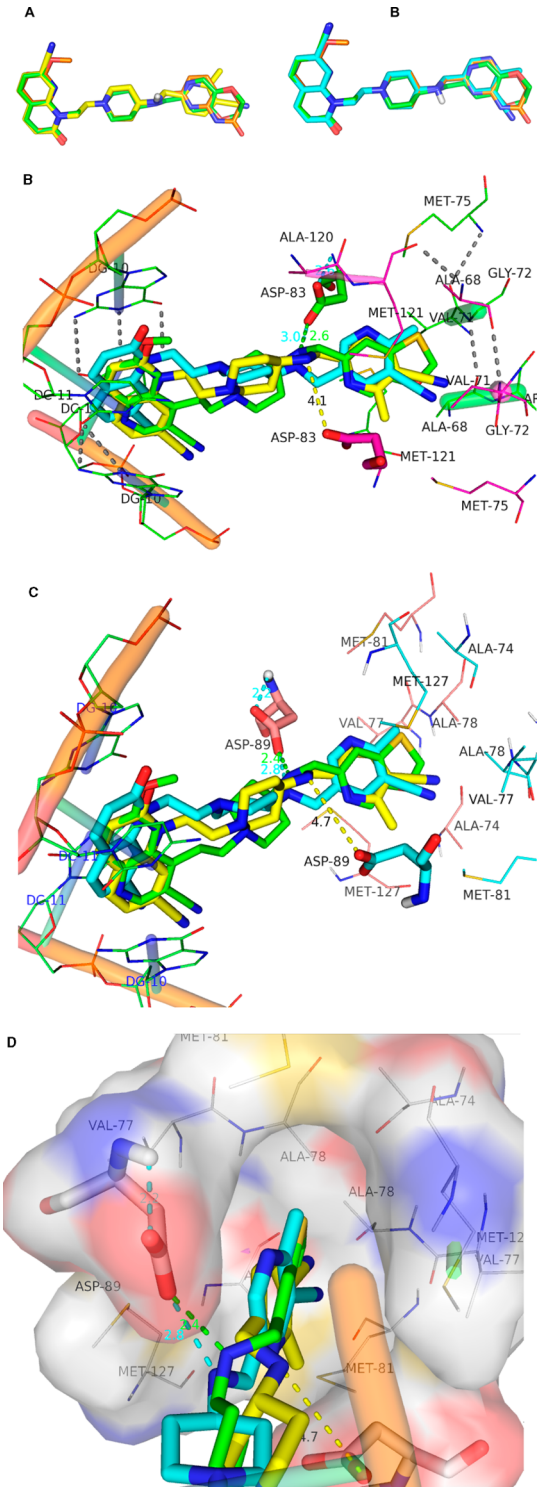

Figure 3. (a) Overlay of the initial leads with compounds containing a novel monocyclic RHS; **4** (yellow) on **1a** (green) and **2a** (orange) (A) and **5** (cyan) on **1a** and **2a** (B). (b) Docking pose of compound **4** (yellow) and **5** (cyan) in the crystal structure of *S. aureus* DNA gyrase bound to **4a** (green).[8a] (c) Docking pose of compound **4** (yellow) and **5** (cyan) on to the homology model of Mtb DNA gyrase subunit A. (d) Molecular surface of the active site depicting the RHS of compound **4** and **5**. The LHS part is not shown in part d for clarity purposes.

group of Asp83 of the *S. aureus* DNA bound GyrA (Asp 89 in Mtb GyrA). This observation was consistent with the binding

dx.doi.org/10.1021/jm500432n | J. Med. Chem. XXXX, XXX, XXX−XXX

mode of **4a**.[8a] On the other hand, the −NH group's hydrogen in compound **4** was 4.1 Å away from the oxygen atom of the carboxylate group in Asp83 (in the homology model of Mtb GyrA, it was 4.7 Å away from Asp89), which is unlikely to make a strong hydrogen-bonding interaction with the Asp83 residue. Thus, the combination of loss of hydrophobic interaction and a weak hydrogen-bonding contact with the Asp 83 may partially explain the loss of potency for compound **4**.

Compounds **4** and **5** also displayed improved Caco-2 permeability over the bicyclic RHS analogue (**1a**, **2a**, and **2b**). Although, compounds **4** and **5** had similar log *D* (1.1−1.3), compound **5** showed moderate hERG inhibition (IC_{50} = 26 μM), whereas compound **4** was more potent (hERG IC_{50} = 5.3 μM) against the hERG channel. The improved hERG selectivity seen for compound **5** could be due to the substitution pattern of CH_3 and cyano groups on the RHS ring. On the basis of the promising profile of compound **5**, we fixed 2-methyl-3-cyanopyridine as the RHS and started exploring the SAR on the LHS. Replacement of the LHS cyanoquinolone ring with 1,5-naphthyridone resulted in a 2−3-fold improvement in the hERG liability, while maintaining the MIC and Caco-2 permeability (compounds **6** and **7** in Table 2). Compound **7** showed a 4-fold improvement in MIC (0.06 μg/mL) as compared to the starting lead **2a**. Moving the methoxy group to the 6-position of the LHS 1,5-naphthyridone weakened the MIC (compounds **7** and **7a** shown as a match pair in Table2), whereas converting compound **7a** to a 1,5-naphthyridinedione form (compound **8**) completely abolished the antimycobacterial activity, suggesting that the substitution at the 7-position of the LHS ring was essential for retaining MIC. The replacement of the 1,5-naphthyridone LHS ring with a 5-cyano-7-methoxyquinolone (compound **9**) improved the Mtb MIC to 0.01 μg/mL at the cost of hERG selectivity. The best MIC observed for compound **9** could be due to the improved binding to enzyme (supercoiling assay IC_{50} = 0.065 μM) or better cell permeability driven by higher lipophilicity. Changing the alkyl bridge of the RHS into an amide was tolerated for both the Mtb MIC and hERG selectivity (compound **7** vs **10** in Table 2). Introduction of additional nitrogen in the RHS ring (pyridine to pyrazine) retained the hERG IC_{50} but weakened the MIC by 15-fold (compound **7** versus **12** in Table 2).

To further improve the hERG selectivity, we explored a pyridopyrazinone ring on the LHS (compounds **13** and **14** in Table 2). Compound **14** with a pyrido[2,3-*b*]pyrazin-2(1*H*)-one improved the hERG inhibition (IC_{50} > 100 μM), and compound **13** with a pyrido[2,3-*b*]pyrazin-3(4H)-one lost the hERG selectivity (IC_{50} = 13 μM). The higher hERG potency observed for compound **13** could be due to the high log *D* and the enhanced π-stacking interaction with the hERG channel. Overall, the reduction of hERG liability for this series tracked well with reduced lipophilicity (lower log *D*) as reported earlier for the antibacterial N-linked aminopiperidine series.[10]

Modulation of the pK_a of aminopiperidine linker through a substitution at the 3-position of piperidine moiety with fluoro substitution lowered the hERG inhibition.[11] Adopting a similar strategy, a 2−3-fold improvement in hERG inhibition was achieved by introducing a fluoro or methoxy group at the 3-position of the aminopiperidine in cis configuration (compounds **15**−**18** in Table 3). The compounds with trans configuration were not synthesized due to synthetic complexity. It was interesting to note that that the linker modification did not affect Mtb MIC and the Caco-2 permeability. Replacing the monocyclic pyridine RHS with a bicyclic RHS along with a fluoro-substituted linker also showed a similar trend in the hERG selectivity (Table 3) without compromising the Mtb MIC. It was also observed that a fluoro-substituted linker modification with a combination of pyridoxazinone RHS and 6-fluoro 1,5-naphthyridone LHS retained the Caco-2 permeability (**19** and **20** in Table 2). This could be due to the better permeability of the fluoro-substituted linker and the LHS part.

Table 2. SAR Modification around RHS and LHS Fragments

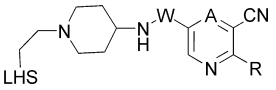

Compound	LHS	R & W	A	Mtb MIC (μg/ml)	Log D	hERG IC_{50} (μM)	Caco-2: Papp A−B/B−A (1×10^{-6} cm/s)
6	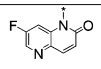	R=CH_3 W=CH_2	CH	0.25	0.81	69	18/9.8
7	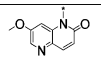	R=CH_3 W=CH_2	CH	0.06	1.07	50.6	10.5/8.3
7a	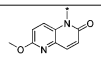	R=CH_3 W=CH_2	CH	4	ND	10	ND[a]
8	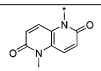	R=CH_3 W=CH_2	CH	>32	-0.6	>33	ND[a]
9	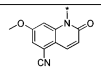	R=CH_3 W=CH_2	CH	0.01	1.86	2.5	10/4.7
10	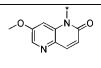	R=CH_3 W=C=O	CH	0.13	1.4	74	4.2/13
11	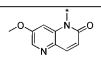	R=OCH_3 W=CH_2	CH	0.06	1.2	12	13/9
12	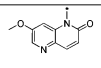	R=CH_3 W=CH_2	N	0.5	0.89	69	ND[a]
13	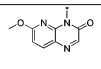	R=CH_3 W=CH_2	CH	0.13	1.65	13	ND[a]
14	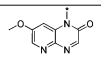	R=CH_3 W=CH_2	CH	0.13	0.38	>100	ND[a]

[a]Not determined.

Structure−Property Relationship for the in Vivo Clearance and Oral Bioavailability in Rats. In general, a majority of compounds from this series showed good solubility (>1000 μM) at pH 7.4. The initial lead compound **2b** with a bicyclic RHS fragment showed 11% oral bioavailability in rats, probably due to poor Caco-2 permeability and high clearance. High clearance for compound **2b** (~2.5 times higher than rat liver blood flow) suggested an extrahepatic route of elimination in the rats (Table 4). Replacement of the bicyclic RHS fragment with a monocyclic 2-methyl-3-cyanopyridine fragment in compounds **5** and **9** improved the oral bioavailability. Replacing the quinolone LHS ring with 1,5-naphthyridone and introduction of a fluoro substitution in the linker region also showed a similar trend (compounds **7**, **16**, and **17** in Table 4).

dx.doi.org/10.1021/jm500432n | J. Med. Chem. XXXX, XXX, XXX−XXX

Table 3. SAR around Linker Modification

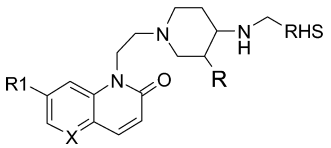

Compound	R1 &X	R	RHS	Mtb MIC (μg/ml)	Log D	hERG IC_{50} (μM)	Caco-2: Papp A−B/B−A (1×10^{-6} cm/s)
15	R1=CN X=CH	F(3S, 4R)	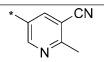	0.25	1.29	>100	14.5/13
16	R1=F X=N	F(3S, 4R)	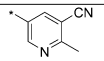	0.25	0.92	133	17.7/15.4
17	R1=OCH3 X=N	F(3S, 4R)	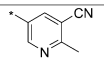	0.06	1.29	90	13.6/7.4
18	R1=OCH3 X=N	OCH_3 (3S,4R)	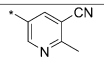	0.06	0.99	151	11.7/9.9
19	R1=F X=N	F(3S, 4R)	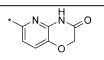	0.13	0.47	>100	7.6/11.2
20	R1=F X=N	F(3R, 4S)	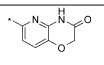	0.13	0.47	>100	8.1/12.3
21	R1=OCH_3 X=N	F(3S, 4R)	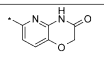	0.03	0.64	>100	4.1/10.8
22	R1=OCH_3 X=N	F(3R, 4S)	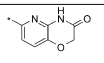	0.06	0.82	>100	3.4/12.7
23	R1=OCH_3 X=N	OCH_3 (3S,4R)	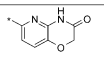	0.13	0.4	>100	ND[a]

[a]Not determined.

Table 4. SPR for Oral Bioavailability

compd	log *D*	PSA (Å^2)	Caco-2: Papp A−B/B−A (1×10^{-6} cm/s)	rat clearance (mL/min/kg)	rat *F* (%)
2b	0.4	105	2.0/12.6	187	11
5	1.31	82	13.6/7.4	41	>100
9	1.71	91	10/4.7	10	59
7	1.07	83	10.5/8.3	32	>100
16	0.92	74	17.7/15.4	30	>100
17	1.29	83	13.6/7.4	42	52
18	0.99	92	11.7/9.9	54	73
20	0.47	97	AB:8.1 BA:12.3	63	>100
19	0.47	97	7.6/11.2	87	87

The methoxy substitution in the aminopiperidine linker with a monocyclic RHS (compound **18**) showed moderate clearance with good bioavailability (73%). Modification of the bicyclic pyrido-oxazinone RHS with 1,5-napthyridone and a fluoro linker combination resulted in moderate to high in vivo clearance with >50% oral bioavailability (compound **19** and **20** Table 4). Good bioavailability (>50%) of compounds **17**−**20** with moderate to high clearance could be due to the saturation of clearance mechanism.

Mechanism of DNA Gyrase Inhibition. In order to understand the mechanism of inhibition at a molecular level vis-a-vis the fluoroquinolones, few representative compounds were tested in the Mtb DNA gyrase supercoiling assay (Table 5) and the cleavable complex assay (Figure 4). Most of the compounds with MIC against Mtb also inhibited the supercoiling activity of Mtb gyrase, thus confirming their mode of inhibition.

Table 5. Aminopiperidines Inhibit the Mtb Gyrase Supercoiling Activity

compd	Mtb gyrase supercoiling IC_{50} (μM)	Mtb MIC (μg/mL)
2b	0.11	0.13
5	0.25	0.06
7	0.14	0.06
9	0.065	0.01
17	0.25	0.06
19	0.35	0.13
20	0.24	0.13
22	0.17	0.1
moxifloxacin	12.5	0.06

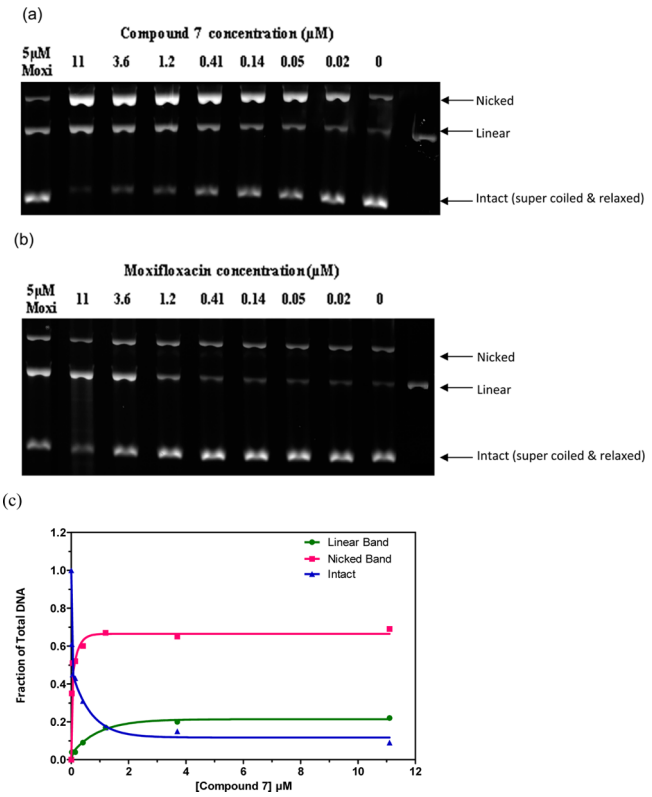

Figure 4. Mtb DNA gyrase cleavable complex assay for (a) compound **7** and (b) moxifloxacin. A titration was performed with varying concentrations of compound **7** and moxifloxacin. (c) Plot representing the relative fractions of nicked, linear, and supercoiled DNA to the total DNA in the sample is shown.

FQs trap the DNA gyrase bound to double-strand cleaved DNA in a ternary complex, thereby resulting in the formation of linearized DNA in the cleavable complex assay, as shown with moxifloxacin (Figure 4b). In contrast, the titration of compound **7** showed an increased formation of single-strand cleaved (nicked) plasmid with increasing compound concentration (Figure 4a,c). We propose that the chemical scaffold described in our work arrests the reaction at the single-strand cleavage (or nick) and, hence, is the primary mode of inhibition

dx.doi.org/10.1021/jm500432n | J. Med. Chem. XXXX, XXX, XXX−XXX

by trapping this as ~70% of reaction product. A small fraction of the enzyme–DNA complex may "proceed" through to the double-stranded cleavage, thereby resulting in a linear product as visualized on the gel. This level, one must note, is rather small (20%), just above the basal level of 10% of intact DNA. A much smaller increase in the formation of linear DNA was seen primarily at lower concentrations, which saturated at 20% of the total DNA in the reaction (basal level of intact DNA ~ 10%). This suggests that the primary mechanism of inhibition of the enzyme–DNA complex by compound **7** appears to be via trapping the transiently single-strand cleaved DNA as it represents ~70% of product formed. This is different from the mechanism of inhibition of FQs which form in classical "cleavable complex".

Another phenomenon observed was that these inhibitors were equipotent in inhibition of the enzyme (IC_{50}) and bacterial cell growth (MIC) as compared to the FQs (e.g., moxifloxacin), which exhibit MIC several orders of magnitude lower than the enzyme inhibition. This phenomenon observed with the FQs has been explained by the downstream effects of double-stranded lesions in the chromosomal DNA, resulting in an SOS response of the cell leading to a more rapid inhibition/kill. This data suggests that the mechanism of action of the N-linked aminopiperidinyl alkyl quinolones and naphthyridones inhibitors could be different from that of the FQs.

Bactericidal Activity of Aminopiperidines against Replicating Mtb in Broth and Macrophages. Detailed time course kill studies were performed to understand the influence of varying drug concentrations over a period of 10 days. As shown in Figure 5a, compounds **19** and **20** displayed a

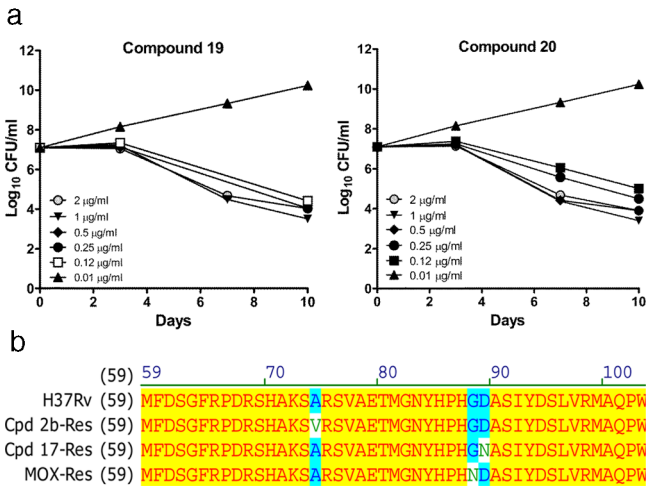

Figure 5. (a) Compounds **19** and **20** display a concentration-dependent as well as time-dependent killing of replicating Mtb grown in broth. (b) In vitro resistance to aminopiperidines (**2b**, **17**) maps to the *gyrA* gene in Mtb.

>3-log reduction in the colony forming units (cfu) over a period of 10 days. The extent of kill increased with both the concentration and time, a property displayed by fluoroquinolones against Mtb.[17] Furthermore, to probe the activity of this series against slowly replicating Mtb residing inside human macrophages, adherent THP-1 macrophages infected with Mtb were exposed to different compounds at a concentration of 1 μg/mL for 7 days at 37 °C, as described earlier.[18b] The representative compounds (**17**, **19**, and **22**) from this series displayed a ~1.3 log kill as compared to the untreated control. Moxifloxacin, used as a positive control, showed ~2.3 log kill at 1 μg/mL. This data highlight the cidality of this compound series against a physiologically relevant intracellular milieu believed to be important in the pathogenesis of tuberculosis.

In order to measure the resistance frequency, spontaneously resistant mutants of Mtb were selected on agar plates containing varying concentrations of compounds **2b** and **17** (Table 6). Mutants resistant to compound **2b** arose at a

Table 6. Aminopiperidines Display a Low Frequency of Spontaneous Resistance against Mtb

compd	Mtb MIC (μg/mL)	mutant selection concn (μg/mL)	mutation frequency
2b	0.13	0.5	2.9×10^{-6}
2b	0.13	1	8.2×10^{-7}
17	0.06	0.5	3.5×10^{-8}
17	0.06	1	8.7×10^{-9}
ciprofloxacin	0.5	4	1.9×10^{-7}
ciprofloxacin	0.5	8	1.9×10^{-7}
moxifloxacin	0.06	0.25	2.6×10^{-8}
moxifloxacin	0.06	0.5	2.3×10^{-8}

frequency of 8.2×10^{-7} at 8× MIC as compared to 2×10^{-7} seen for ciprofloxacin at 8× MIC. In contrast, mutants resistant to compound **17** arose at a frequency of 3.5×10^{-8} at ~10× MIC (8.7×10^{-9} at ~20× MIC), which is similar to the observed frequency for moxifloxacin (2.3×10^{-8}) at a similar multiples of the MIC.

Compounds from this series were tested for their MIC against resistant mutants selected using **2b**, **17**, and moxifloxacin. As shown in Table 7, compounds **2b** and **17**, as

Table 7. MIC of Aminopiperidine against Mutants Resistant to Compound 2b and 17

	MIC (μg/mL)			
compd	Mtb H37Rv wild-type	compd **2b**^{R} mutant (A74V)	compd **17**^{R} mutant (D89N)	Moxi^R mutant (G88N)
2b	0.13	2	>2	0.03
17	0.06	1	>1	0.03
5	0.06	>2	>2	0.06
20	0.13	>2	>2	0.06
moxifloxacin	0.06	0.06	1	4
ciprofloxacin	0.25	0.25	4	8
ofloxacin	0.5	1	4	16
isoniazid	0.06	0.06	0.03	0.06
rifampicin	0.015	0.008	0.015	0.008

well as other analogues, showed a ≥16-fold increase in MIC (compared to the wild-type H37Rv strain) to the **2b**- or **17**-resistant mutant strains, while showing no change in their MIC against the moxifloxacin-resistant isolate. Interestingly, moxifloxacin retained its wild-type MIC against the compound **2b**-resistant clone, but its MIC increased ~16 times versus the compound **17**-resistant clone. Ciprofloxacin and ofloxacin retained their MIC on the **2b**-resistant clone, but their MIC increased 16 and 8 times against the **17**-resistant clone. The aminopiperidines retained their MIC against moxifloxacin-resistant mutants, whereas MIC for three FQs increased by >16-fold (Table 7). Isoniazid and rifampicin retained their wild-type MIC against all the resistant clones tested; indicating that

dx.doi.org/10.1021/jm500432n | J. Med. Chem. XXXX, XXX, XXX–XXX

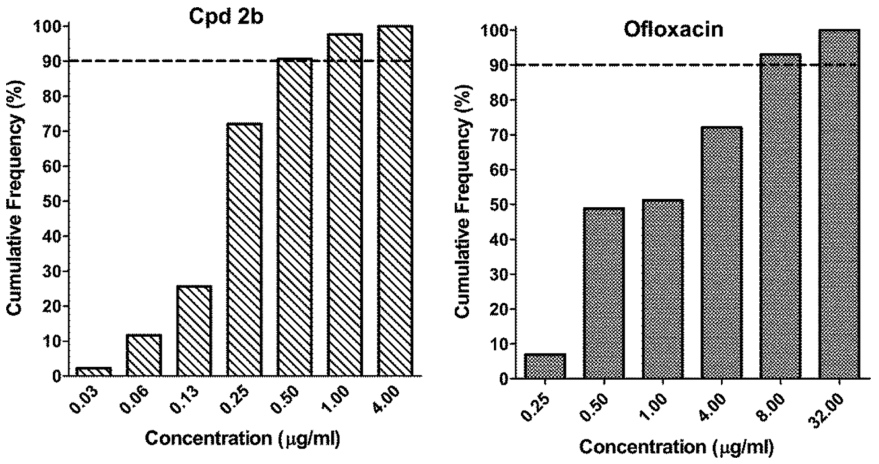

Figure 6. Aminopiperidines (**2b**) retain their MIC against a diverse panel of clinical isolates of Mtb. Cumulative frequency is defined as the sum of all previous frequencies up to the current point.

the resistant clones had a specific mutation in the gyrase gene. The entire *gyrA* gene of six spontaneous resistant clones from each compound were sequenced. The multiple sequence alignment of the mutated and the wild-type genes confirmed mutations in the *gyrA* gene. These mutations were clustered around the N-terminal domain of the GyrA protein spanning amino acid position 74−104. Mutants resistant to **2b** had a A74V amino acid change. Interestingly, the **17**-resistant clone 16.4 showed a different mutation: D89N in the vicinity of the amino acid 88, which is critical for mediating resistance to moxifloxacin.[22] The mutation in the moxifloxacin resistant clone was G88N, which is consistent with the earlier observation that moxifloxacin resistance maps to G88N in the laboratory setting as well as in the clinic.[22]

Furthermore, to prove that the novel mechanism of action of aminopiperidines is relevant in the clinic, we tested compound **2b** against a panel 44 clinical isolates of Mtb using an agar plate dilution method, as described earlier.[24] This panel included 22 strains of Mtb that were fully susceptible to FQs and 22 strains resistant to FQs. As shown in Figure 6, compound **2b** retained its wild-type MIC_{90} (<0.5 μg/mL) against all the 44 clinical isolates, irrespective of their susceptibility pattern to FQs. On the contrary, the MIC_{90} of ofloxacin shifted significantly from 0.25 to >8 μg/mL. This data clearly highlights the potential of the aminopiperidines in the treatment of multidrug-resistant TB, which is steadily increasing in numbers across the globe.[2]

In Vivo Efficacy and Pharmacokinetic and Pharmacodynamic (PK−PD) Relationship. Several compounds with good MIC, cidality, and pharmacokinetic profile were selected for establishing the in vivo proof of concept in a murine model of TB and understanding the PK−PD relationship for this series. The PK profile in healthy mice suggested that the treatment with ABT before giving the first dose and twice daily dosing were essential to maintain adequate plasma concentrations of the compound to drive efficacy. The data for five compounds, representing both monocyclic and bicyclic RHS, tested in the acute murine model of TB are shown in Figure 7A. Compound **7** with a monocyclic RHS showed the best efficacy. It reduced the bacterial burden in lungs to below the limit of quantification at 20 mg/kg dose. Compounds with a bicyclic RHS were relatively less efficacious (**19**, **20**, and **22**). The best efficacy in this class was observed for compound **19**: a 1.2 log reduction in the bacterial cfu at 160 mg/kg. Similarly, in the chronic model of mouse TB (Figure 7B), ∼0.5 log reduction in lung cfu was observed at 40 or 80 mg/kg dose of compounds **5** and **7** (monocyclic RHS) as compared to 240 mg/kg dose of compound **22** (bicyclic RHS). The percentage time of dosing interval for free plasma concentration to be above the MIC was >50 for all the compounds profiled (Table 8). However, the free AUC/MIC ratio for compound **7** was nearly 8 times lower than for compound **22**. The efficacy for compounds **5** and **7** in the chronic model improved significantly with an extended duration of treatment (Figure 7C).

CONCLUSION

In summary, screening of a focused antibacterial library followed by a lead optimization effort led to the identification of a novel class of N-linked aminopiperidine-based alkyl quinolone and naphthyridone compounds with excellent Mtb MIC, improved pharmacokinetic properties, and significantly reduced hERG liability. These compounds inhibited the Mtb DNA gyrase with a novel mode of inhibition that conferred the ability to retain their MIC against FQ-resistant clinical isolates of Mtb. Compound **7** with monocyclic RHS and compound **19** with bicyclic RHS displayed the best efficacy in the acute model of TB. Compound **5** and **7** were also efficacious in the chronic model of TB. Our lead optimization efforts led to a significant improvement in the properties that are suitable for an oral route of administration. Additionally, the medicinal chemistry efforts have provided enough structural diversity to optimize the safety and pharmacokinetic properties of this series. In conclusion, the N-linked aminopiperidine lead series represents an attractive class of gyrase inhibitors with the potential to treat drug-susceptible as well as drug-resistant TB, including FQ-resistant TB. Assessment of the in vivo safety is essential before optimizing this class of compounds toward the development of a novel anti-TB drug.

EXPERIMENTAL SECTION

Computational Methods. *Ligand Preparation.* Throughout the studies, CORINA (http://www.molecular-networks.com/products/corina) was used for generating 3D structures from smiles, and Omega 2.2.0 (OpenEye Scientific Software, Santa Fe, NM 87507) was used for generating conformers. Default settings were retained for both the tools.

*Molecular Alignment of Compounds **4** and **5**.* ROCS, a shape-based molecular alignment tool (Version 3.2, OpenEye Scientific Software) was used for molecular alignment. Shape Tanimoto score

dx.doi.org/10.1021/jm500432n | J. Med. Chem. XXXX, XXX, XXX−XXX

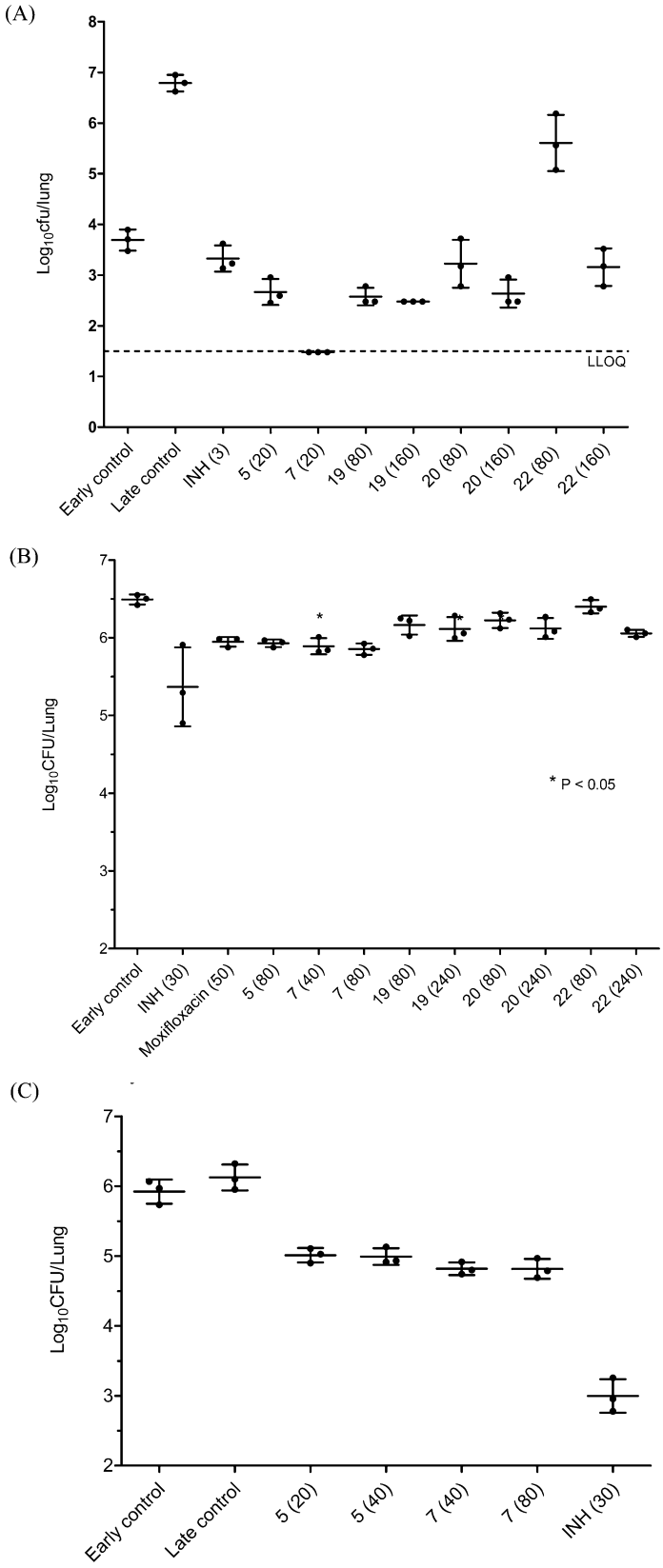

Figure 7. Efficacy after 20 days of daily treatment with compound **5**, **7**, **19**, **20**, and **22** in the acute model (A) or chronic (B) model and when treatment was given for 8 weeks (6 days/week) in the chronic model (C). Numbers in the bracket indicate the dose (mg/kg). The dotted line indicates the lower limit of quantitation (LLOQ) for the lung cfu. The mean and standard deviation are shown for each dose group.

was used to rank the overlays. The omega-generated multiconformers (max number of output conformers per molecule = 30) of compound **1a** and **2a** were aligned to the crystal-bound conformation of **4a** (PDB ID 2XCS). The best scoring conformation of compounds **1a** and **2a**

dx.doi.org/10.1021/jm500432n | J. Med. Chem. XXXX, XXX, XXX–XXX

Table 8. Pharmacokinetic and Pharmacodynamic Parameters in Mice

compd	MIC (μg/mL)	fraction unbound in mouse plasma	dose (mg/kg)	free AUC/MIC	% free T > MIC
5	0.062	0.43	20	159	58
7	0.062	0.23	20	54	58
19	0.125	0.32	80	129	70
20	0.125	0.44	80	175	58
22	0.062	0.48	160	434	83

was further utilized as reference to derive the best possible conformer of compounds **4** and **5** from the pool of multiple conformers.

Homology Modeling. *Mycobacterium tuberculosis* gyrase subunit A (Mtb GyrA) was built by homology modeling using MOE (Molecular Operating Environment, Version 2013.12, Chemical Computing Group, Montreal, Canada). The published *S. aureus* DNA gyrase subunit A (Sau GyrA) crystal structure was retrieved from Protein Data Bank (PDB ID 2XCS 2.1 Å) and examined for (1) ligand interaction and followed by (2) similarity with Mtb GyrA.

The NBTI binds to a site adjacent to the FQ binding site (Figure 13 in Supporting Information) as evident in the published crystal structure.[8a] The NBTI binds midway between the two active sites, with the quinoline-carbonitrile group sitting in between the two central base pairs of the stretched DNA and the oxathiolopyridine group occupying the noncatalytic pocket that opens up between the two GyrA subunits[8a] (refer to ref 8a for further details).

Overall primary sequence similarity of Mtb with Sau GyrA was found to be 42%, whereas the active site similarity was >95% (Figure 8 in Supporting Information), and thus Sau GyrA served as template for the Mtb GyrA model generation [GeneDoc Ver 2.6.002 (http://www.nrbsc.org/gfx/genedoc/) with default options was used for multiple alignments of sequences].

Model Generation Steps. Ten different models of Mtb GyrA were generated with the default settings as implemented in MOE. The bound ligand and DNA were used as the environment for induced fit. Out of the 10 different models, the model with lowest RMSD (C-α) to the average position of all of the intermediate models was selected. Analysis of the Ramachandran plot of the selected model indicated that >95% of the residues were in the allowed region. The coordinates of DNA and the ligand from the 2XCS structure were merged into the homology model of Mtb GyrA. The resultant complex of model was further analyzed and minimized in Maestro (version 8; Schrödinger, LLC) using default parameters of the Protein Preparation Tool. The RMSD (C-α) of the Mtb GyrA model and Sau GyrA was found be less than 2 Å. No major structural differences were observed between the Mtb GyrA model and Sau GyrA crystal structure and the overall architecture remains the same (Figure 9 in Supporting Information). The active site (5 Å radius from ligand, 2XCS) is very well conserved, except that Gly72 of Sau GyrA is occupied by Ala78 in Mtb GyrA. This difference is not disturbing the architecture of the active site and provides additional hydrophobicity to the active site of Mtb GyrA (Figure 10 in Supporting Information). The energy-minimized model was used for docking.

Molecular Docking. Molecular dockings into the Sau GyrA and Mtb GyrA model were performed using FRED (Version 2, OpenEye Scientific Software). The Receptor Tool in FRED was used to prepare the receptor input file for docking. The active site was defined by selecting the ligand and a docking constrain involving Asp83/89 of Sau and Mtb GyrA as a hydrogen bond acceptor was added. The Asp was found to be involved in critical hydrogen bond interaction with the ligand and mutation of it was found to affect the activity of NBTIs.[8a] The docking protocol was validated by extracting the bound conformation of the ligand and redocking into the receptor. The best agreement was found between docked pose and crystal bound conformation (RMSD < 0.8 Å in both the receptor). After this validation, the receptor was used for docking. Apart from the default Chemgauss3 scoring function, CGO scoring (based on the shape overlay of ligands) was used.

The docking of designed molecules was done in two steps. In the first step the multiple conformers of the compound to be docked were aligned using ROCS onto the best-aligned conformation of compound **2a** onto the crystal ligand. A maximum of five conformations per compound were opted as an output from ROCS. In the second step the resultant conformations of designed compounds were docked using the FRED protocol as described above. Consensus scoring and visual inspection were used to select the pose. The complex of selected pose and protein was subjected to constrained minimization using Macromodel (Schrodinger) and the OPLS force field to remove unfavorable contacts.

Determining the Antimycobacterial Properties. Mtb H37Rv ATCC 27294 was used for all the studies and was grown and tested as described earlier.[23] The minimum inhibitory concentration (MIC) was determined as described earlier.[18b]

Cleavable Complex Assay with Mtb H37Rv Gyrase Holoenzyme. The cleavable complex assay was performed in 96-well PCR plates (Bio-Rad) in 30 μL volume. The assay mix contained 400 nM of −Mtb H37Rv holoenzyme, 105 ng of relaxed pBR322 DNA, 40 mM HEPES−KOH pH 7.5, 100 mM potassium glutamate, 25 mM KCl, 1 mM spermidine, 10 mM $MgCl_2$, 4 mM DTT, 6% glycerol, and 0.35 mg/mL BSA. The assay was started with the addition of DNA and carried out for 60 min at 37 °C. The reaction was stopped by addition of 0.75 μL of proteinase K (20 mg/mL, 40 U/mg) and 3 μL of 2% SDS followed by incubation at 37 °C for 1 h. This was followed by the addition of 4 μL of 10× DNA-loading dye to samples followed by loading onto the gel. Nicked, linear, and supercoiled forms of DNA were separated by gel electrophoresis for 16 h at 1 V/cm, on a 0.8% agarose in buffer containing 45 mM Tris−borate, 1 mM EDTA, and 0.3 μg/mL ethidium bromide. An image of the gel was captured using a Fujifilm FLA 5100 Phosphorimager and used for quantitation of the DNA using Bio-Rad's Quantity One software.

Determination of IC_{50} for the Supercoiling Activity of Mtb H37Rv Gyrase Holoenzyme. DNA supercoiling assay was performed in 96-well PCR plates (Bio-Rad) in 30 μL volume. Assay mix contained 12.5 nM Mtb H37Rv holoenzyme, 50 ng of relaxed pBR322 DNA, 40 mM HEPES−KOH pH 7.5, 100 mM potassium glutamate, 15 mM KCl, 1 mM spermidine, 10 mM $MgCl_2$, 4 mM DTT, 8% glycerol, 0.36 mg/mL BSA, and 75 μM ATP. The assay was started with the addition of DNA and ATP mix and continued for 90 min at 37 °C. The reaction was stopped by addition of 0.75 μL of Proteinase K (20 mg/mL, 40 U/mg) and 3 μL of 2% SDS followed by incubation at 37 °C for 1 h. This was followed by the addition of 4 μL of 10× DNA-loading dye to samples followed by loading onto the gel. Supercoiled and relaxed forms of DNA were separated by gel electrophoresis for 16 h at 1 V/cm, on a 0.8% agarose in buffer containing 45 mM Tris−borate and 1 mM EDTA. The gel was stained for 10 min with a solution containing 0.7 μg/mL ethidium bromide in water and destained in water for 30 min, followed by imaging and quantitation of the gel bands.

Time Kill Studies against Mtb in 7H9 Broth. This assay was performed in a 200 μL volume using 96-well microplates with Middlebrook 7H9 broth supplemented with 0.2% glycerol, 0.05% Tween 80 (Sigma), and 10% albumin dextrose catalase (Difco Laboratories, Detroit, MI) as described earlier.[18b] Serial 2-fold dilutions of aminopiperidines spanning a wide concentration range were added to each of the 96-wells containing approximately 3×10^7 cfu/mL of Mtb H37Rv. The plates were incubated at 37 °C. Bacterial enumeration was performed on Middlebrook 7H11 agar plates at 0, 3, 7, and 10 days after drug exposure. The plates were incubated for up to 28 days at 37 °C, in 5% CO_2 in a humidified atmosphere. The bacterial colonies were enumerated and data expressed as the $\log_{10}$ cfu for each drug concentration.

Determination of Resistance Frequency. Spontaneous resistant mutants were raised against compound **2b**, **17**, ciprofloxacin, and moxifloxacin using a single step selection method as described.[19] Briefly, a mid-logarithmic phase culture of Mtb H37Rv was centrifuged and concentrated 100-fold to achieve a bacterial number of $\sim 10^{10}$ cfu/mL. Varying dilutions of the bacterial culture were plated onto

dx.doi.org/10.1021/jm500432n | J. Med. Chem. XXXX, XXX, XXX−XXX

compound-containing plates. Appropriate dilutions of the bacterial culture were also plated on drug-free Middlebrook 7H11 agar to enumerate the bacterial numbers in the culture. Plates were incubated for 4 weeks at 37 °C and the cfu in drug-free plates were enumerated. The drug-containing plates were incubated for up to 6−8 weeks at 37 °C to enumerate the number of resistant colonies.

The spontaneous rate of resistance was calculated by dividing the number of colonies on drug-containing plates (at a given concentration) divided by the total number of viable bacteria estimated on drug-free plates. Resistant colonies were randomly picked from the drug-containing plates and grown in complete 7H9 broth to determine their level of resistance against the parent compound, close analogues, and TB drugs with different mechanisms of action.

Genetic Mapping of Mutations Conferring Resistance to N-Linked Aminopeperidinyl Alkyl Quinolones and Naphthyridones. In order to map the genetic mutations arising following compound exposure and mutant selection, genomic DNA from microbiologically well characterized colonies was isolated. The entire *gyrA* gene of resistant mutants and wild-type Mtb H37Rv were PCR amplified using standard conditions from boiled supernatants using specific Mtb primers to amplify the entire *gyrA* gene. PCR was performed with cycling parameters of 94 °C for 30 s, 60 °C for 30 s, and 72 °C for 2 min for 30 cycles in a DNA Engine Dyad cycler (Bio-Rad). PCR products were purified from the gel (PCR purification kit, Qiagen), quantitated, and sequenced (Microsynth). The sequences from the resistant clones were aligned against the wild-type H37Rv *gyrA* gene using Vector NTI software to detect mutations in the target gene.

In Vivo Studies in Mice. All animal experimentation protocols were approved by the Institutional Animal Ethics Committee registered with the Government of India (Reg. No. 5/1999/CPCSEA). Six to eight week old BALB/c mice, purchased from RCC laboratories, Hyderabad, India, were used in the pharmacokinetic (PK) and pharmacodynamic (PD) studies. Animals randomly assigned to cages were allowed a 2 week acclimatization period before initiating the experiment. Feed and water were given ad libitum.

Pharmacokinetics. PK was analyzed in the infected mice during the efficacy study. Blood samples from infected mice were collected on day 18 or 19 of dosing and processed in a BSL3 laboratory. Compounds **5**, 7, **19**, **20**, and **22** were formulated in a solution containing 5% dextrose, pH adjusted to 4−5 with 5 M acetic acid. Test compounds, or the corresponding vehicle, were orally administered through gavage at 10 mL/kg dose volume. Aminobenzotriazole (ABT), a known cytochrome P450 inhibitor, dissolved in water, was orally administered at a dose of 100 mg/kg (10 mL/kg) 2 h before dosing the compound to reduce the first pass metabolism and increase plasma exposure. Blood samples were collected by puncturing the saphenous vein at 5, 15, and 30 min and 1, 2, 4, and 6 h after dosing. The same formulation as above was used for intravenous PK at 5 mg/kg and per oral PK at 40 mg/kg dose in rats. Plasma samples from mice/rats were mixed with chilled acetonitrile (1:10 v/v) to precipitate proteins, vortexed, and centrifuged at 4000 rpm for 30 min at 10 °C. The resulting supernatant was mixed with mobile phase containing carbamazepine (internal standard, 10 ng/mL) and analyzed for drug concentrations by liquid chromatography with tandem mass spectrometry (LC−MS/MS). Chromatographic separation was achieved on a Gemini C18 column (50 × 4.6 mm, particle size 5 μm, Phenomenex) by isocratic elution with 40% 10 mM ammonium acetate buffer in acetonitrile at 500 μL/min flow rate over 4.5 min. An AB Sciex API3000 triple quadrupole mass spectrometer (Applied Biosystems) equipped with a turbo ionspray source was used for the quantitation. The area under the concentration (AUC) vs time PK profile was calculated by noncompartmental analysis (WinNonLin 5.2.1, Pharsight Inc.).

Pharmacodynamics. BALB/c mice were infected in an aerosol chamber as described earlier.[18d] Infected mice were housed in individually ventilated cages (Allentown Technologies) in a biosafety level (BSL)-3 facility. Treatment was initiated after 3 days and 4 weeks of infection in the acute and chronic model, respectively. Vehicle- or compound-treated groups contained three mice each. An additional three mice were sacrificed just after infection to serve as early controls. Isoniazid was formulated in 0.5% (w/v) (hydroxypropyl)methyl cellulose (HPMC), whereas test compounds were prepared in the same formulation as used for the PK study. ABT was orally administered before compound administration, as described above. In the acute model, infected mice were treated with an oral dose of 20, 40, 80, or 160 mg/kg of compound **5**, 7, **19**, **20**,**22** given twice daily (8 h interval) for 20 days (7 days/week). In the first chronic model efficacy study, infected mice were treated with an oral dose of 40, 80, or 240 mg/kg of compound **5**, 7, **19**, **20**, and **22** given twice daily (8 h interval) for 20 days (7 days/week). In a second chronic model efficacy study, infected mice were treated with an oral dose of 20, 40, or 80 mg/kg of compound **5** or 7 twice daily (8 h interval) for 8 weeks (6 days/week). Mice were sacrificed after completion of treatment and suitable dilutions of lung homogenates were plated on 7H11 agar to determine viable cfu per mouse lung tissue. One-way analysis of variance (ANOVA) followed by the Bonferroni's multiple comparison test was used to analyze efficacy data.

General Chemical Methods. All commercial reagents and solvents were used without further purification. Analytical thin-layer chromatography (TLC) was performed on SiO_2 plates on alumina. Visualization was accomplished by UV irradiation at 254 and 220 nm. Flash column chromatography was performed using the Biotage Isolera flash purification system with SiO_2 60 (particle size 0.040−0.055 mm, 230−400 mesh). The purity of all final derivatives for biological testing was confirmed to be >95%, as determined using the following conditions: a Shimadzu HPLC instrument with a Hamilton reverse-phase column [HxSil, C18, 3 μm, 2.1 mm × 50 mm (H2)]; eluent A, 5% CH_3CN in H_2O; eluent B, 90% CH_3CN in H_2O; a flow rate of 0.2 mL/min was used with UV detection at 254 and 214 nm. The structures of the intermediates and end products were confirmed by ^1H NMR and mass spectroscopy. Proton magnetic resonance spectra were determined in DMSO-d_6, unless otherwise stated, using Bruker DRX-300 or Bruker DRX-400 spectrometers, operating at 300 or 400 MHz, respectively. Splitting patterns are indicated as follows: s, singlet; d, doublet; t, triplet; m, multiplet; br, broad peak. LCMS data were acquired using an Agilent LCMS VL series with ES ionization, coupled with an Agilent 1100 series HPLC system and an Agilent 1100 series PDA as the front end. HRMS data was acquired using an Agilent 6520 quadrupole-time of flight tandem mass spectrometer (Q-Tof MS/MS) coupled with an Agilent 1200 series HPLC system.

The synthesis of compound **1a**, **2a**, and **2b** were previously reported by Reck et al.[10]

1-(2-(4-((5-Cyano-6-methylpyridin-2-yl)methylamino)-piperidin-1-yl)ethyl)-2-oxo-1,2-dihydroquinoline-7-carbonitrile (4). In a 100 mL round-bottomed flask, **27a**[11] (250 mg, 0.84 mmol) and **31** (185 mg, 1.27 mmol) were taken up in a DCE (8 mL) and ethanol (2.000 mL) mixture. Acetic acid (0.050 mL, 0.84 mmol) was added to the reaction mixture that was then heated at 80 °C for 1 h. The reaction mixture was then cooled to rt and then sodium triacetoxyborohydride (536 mg, 2.53 mmol) was added to it portionwise. The reaction mixture was then stirred at rt overnight.

The reaction was monitored by LCMS. The profile showed formation of imine and only 20% product. Sodium cyanoborohydride (106 mg, 1.69 mmol) was added to the reaction mixture and it was stirred at rt for 4 h. The reaction mixture was then evaporated and the residue was then neutralized with saturated $NaHCO_3$. It was then partitioned between DCM (5%MeOH) and water. The organic layer was then separated, dried (Na_2SO_4), and evaporated to get a residue that was then chromatographed with DCM/MeOH to get **4** (75 mg, 20.85%): ^1H NMR (300 MHz, DMSO-d_6) δ1.24 (d, J = 8.85 Hz, 2 H), 1.81 (d, J = 10.74 Hz, 2 H), 2.04 (t, J = 10.55 Hz, 2 H), 2.15 (br s, 1 H), 2.38 (br s, 1 H), 2.51 (s, 3 H), 2.55 (br s, 2 H), 2.92 (d, J = 11.11 Hz, 2 H), 3.76 (br s, 2 H), 4.37 (t, J = 6.50 Hz, 2 H), 6.79 (d, J = 9.42 Hz, 1 H), 7.66 (d, J = 8.10 Hz, 1 H), 7.84 (d, J = 7.72 Hz, 1 H), 7.93 (t, J = 8.29 Hz, 2 H), 8.01 (d, J = 9.61 Hz, 1 H), 8.09 (s, 1 H); HRMS m/z (ES+) 427.217 21 (MH^+) for $C_{25}H_{26}N_6O$.

1-(2-(4-((5-Cyano-6-methylpyridin-3-yl)methylamino)-piperidin-1-yl)ethyl)-2-oxo-1,2-dihydroquinoline-7-carboni-

trile (5). In a 500 mL round-bottomed flask, **27a** (11 g, 37.12 mmol) and sodium carbonate monohydrate (13.81 g, 111.35 mmol) were taken up in DMF (100 mL). In another liquid addition funnel **32** (8.40 g, 37.12 mmol) was taken up in DMF (100 mL), and the solution was then added slowly to the above reaction mixture. The reaction mixture was then stirred at rt for 4 h. The solvent was evaporated to dryness and the residue was then partitioned between DCM (5% MeOH) and water. The organic layer was then separated, dried, and chromatographed with DCM/MEOH to get a slightly crude product. The solid was then triturated in succession with DCM/hexane and MeOH/ether to get slightly impure **5** (9.30 g, 58.7%), which was again triturated with water/MeOH to get 4.85 g of pure compound. The remaining amount was later purified by preparative HPLC to get another 1.577 g of product: ^{1}H NMR (300 MHz, DMSO-d_6) δ 1.20 (d, J = 12.43 Hz, 3 H), 1.76 (d, J = 11.87 Hz, 2 H), 1.92−2.11 (m, 2 H), 2.30 (d, J = 14.51 Hz, 2 H), 2.54 (br s, 1 H), 2.65 (s, 3 H), 2.90 (d, J = 11.68 Hz, 2 H), 3.74 (s, 2 H), 4.36 (t, J = 6.59 Hz, 2 H), 6.78 (d, J = 9.42 Hz, 1 H), 7.65 (d, J = 7.91 Hz, 1 H), 7.91 (d, J = 8.10 Hz, 1 H), 8.00 (d, J = 9.61 Hz, 1 H), 8.08 (s, 1 H), 8.15 (d, J = 1.88 Hz, 1 H), 8.66 (d, J = 1.88 Hz, 1 H); HRMS m/z (ES+) 427.225 70 (MH^+) for $C_{25}H_{26}N_6O$.

5-((1-(2-(7-Fluoro-2-oxo-1,5-naphthyridin-1(2*H*)-yl)ethyl)-piperidin-4-ylamino)methyl)-2-methylnicotinonitrile (6). In a 100 mL round-bottomed flask, **27b** (1.500 g, 5.17 mmol), **32** (1.286 g, 5.68 mmol), and sodium carbonate (1.095 g, 10.33 mmol) were taken up in DMF (25 mL) to give a yellowish solution under nitrogen atmosphere that was heated to 70 °C for 1 h. Solvent was evaporated from the reaction mixture. Water was added to it and extracted using 10% methanol in DCM (4 × 25 mL). The combined organic layers were concentrated to dryness and purified by silica gel chromatography using 0−18% methanol in DCM to yield **6** (1.400 g, 64.4%) as brown solid; 200 mg of the product was purified by preparative HPLC to obtain product as the diacetate salt: ^{1}H NMR (300 MHz, DMSO-d_6) δ1.15−1.29 (m, 2 H), 1.73−1.83 (m, 2 H), 1.91 (s, 6 H), 1.97−2.10 (m, 2 H), 2.31−2.43 (m, 1 H), 2.53−2.59 (m, 2 H), 2.65 (s, 3 H), 2.90 (d, J = 11.68 Hz, 3 H), 3.77 (s, 2 H), 4.31 (t, J = 6.59 Hz, 2 H), 6.83 (d, J = 9.80 Hz, 1 H), 7.95 (d, J = 9.80 Hz, 1 H), 8.01 (dd, J = 11.30, 2.07 Hz, 1 H), 8.16 (d, J = 1.88 Hz, 1 H), 8.56 (d, J = 2.45 Hz, 1 H), 8.67 (d, J = 1.88 Hz, 1 H); HRMS m/z (ES+) 421.21490 (MH^+) for $C_{23}H_{25}FN_6O{\cdot}2CH_3COOH$.

5-((1-(2-(7-Methoxy-2-oxo-1,5-naphthyridin-1(2*H*)-yl)ethyl)-piperidin-4-ylamino)methyl)-2-methylnicotinonitrile (7). In a 500 mL round-bottomed flask **6** (6.3 g, 14.98 mmol) was taken up in methanol (100 mL) under N_2. To this mixture was added sodium methoxide (3.24 g, 59.93 mmol) with stirring. The resulting reaction was stirred at 70 °C for 6 h. The reaction was cooled to rt, and solvent was evaporated to dryness. The obtained solid was diluted with water and extracted with 5% methanol in DCM. The organic layer was separated, washed with brine, and dried to get a residue. The residue was then purified on silica with DCM/MeOH to a slightly crude compound, which on trituration with acetonitrile afforded the pure **7** (4.01 g, 61.9%): ^{1}H NMR (300 MHz, DMSO-d_6) δ 1.11−1.32 (m, 2 H), 1.76 (d, J = 10.93 Hz, 2 H), 1.94−2.10 (m, 2 H), 2.28 (d, J = 18.46 Hz, 2 H), 2.54 (br s, 2 H), 2.64 (s, 3 H), 2.91 (d, J = 11.30 Hz, 2 H), 3.34 (s, 2 H), 3.98 (s, 3 H), 4.35 (t, J = 6.78 Hz, 2 H), 6.66 (d, J = 9.80 Hz, 1 H), 7.41 (d, J = 2.26 Hz, 1 H), 7.86 (d, J = 9.61 Hz, 1 H), 8.15 (d, J = 1.88 Hz, 1 H), 8.28 (d, J = 2.26 Hz, 1 H), 8.66 (d, J = 2.07 Hz, 1 H); HRMS m/z (ES+) 433.235 90 (MH^+) for $C_{24}H_{28}N_6O_2$.

5-((1-(2-(6-Methoxy-2-oxo-1,5-naphthyridin-1(2*H*)-yl)ethyl)-piperidin-4-ylamino)methyl)-2-methylnicotinonitrile (7a). In a 100 mL round-bottomed flask, **27c** (800 mg, 2.65 mmol), **32** (658 mg, 2.91 mmol), and sodium carbonate (561 mg, 5.29 mmol) were taken up in DMF (20 mL) to give a yellowish solution under nitrogen atmosphere that was heated to 70 °C for 1 h. Solvent was evaporated from the reaction mixture. Water was added to it and the mixture was extracted using 10% methanol in DCM (3 × 50 mL). The combined organic layers were concentrated to dryness and purified by silica gel chromatography using 0−15% methanol in DCM to obtain an impure product (270 mg) that was repurified by preparative HPLC to yield **7a** (270 mg, 23.59%) as white solid: ^{1}H NMR (300 MHz, DMSO-d_6) δ 1.11−1.33 (m, 2 H), 1.67−1.84 (m, 2 H), 2.01 (t, J = 11.02 Hz, 2 H), 2.18−2.38 (m, 2 H), 2.64 (s, 3 H), 2.79−2.98 (m, 2 H), 3.73 (s, 2 H), 3.91 (s, 3 H), 4.31 (t, J = 6.78 Hz, 2 H), 6.79 (d, J = 9.80 Hz, 1 H), 7.12 (d, J = 9.23 Hz, 1 H), 7.80 (d, J = 9.80 Hz, 1 H), 8.00 (d, J = 9.23 Hz, 1 H), 8.15 (d, J = 1.88 Hz, 1 H), 8.66 (d, J = 1.88 Hz, 1 H); HRMS m/z (ES+) 433.234 27 (MH^+) for $C_{24}H_{28}N_6O_2$.

6-Methoxy-1-methyl-1,5-naphthyridin-2(1*H*)-one (8-ii). In a 100 mL round-bottomed flask, **24c** (2.000 g, 11.35 mmol) and cesium carbonate (4.07 g, 12.49 mmol) were taken up in DMSO (20 mL) to give a tan suspension. Then to this was added methyl iodide (1.065 mL, 17.03 mmol), and the resulting reaction mixture was heated to 60 °C for 2 h. Water was added to the reaction mixture, which was extracted using EtOAc (5 × 50 mL). The resulting organic layers were washed with water, dried over sodium sulfate, and concentrated under vacuum to obtain crude solid. The crude product was purified by silica gel column using 0−9% methanol in DCM to yield **8-ii** (1.800 g, 83%) as solid: ^{1}H NMR (300 MHz, DMSO-d_6) δ 3.61 (s, 3 H), 3.91 (s, 3 H), 6.80 (d, J = 9.61 Hz, 1 H), 7.12 (d, J = 9.23 Hz, 1 H), 7.79 (d, J = 9.61 Hz, 1 H), 8.00 (d, J = 9.04 Hz, 1 H); HRMS m/z (ES+) 191.23 $(M + H)^+$ for $C_{10}H_{10}N_2O_2$.

1-Methyl-1,5-naphthyridine-2,6(1*H*,5*H*)-dione (8-iii). In a 250 mL round-bottomed flask, **8-ii** (1.700 g, 8.94 mmol) was taken up in 48% HBr in water (15 mL, 276.23 mmol) to give a yellow solution. The resulting reaction mass was stirred at 80 °C for 2 h. The reaction mass was concentrated to dryness and the pH was adjusted to ∼7. The yellow solid obtained was filtered, washed with hexane, and dried to yield **8-iii** (1.800 g, 114%) as yellow solid: ^{1}H NMR (300 MHz, DMSO-d_6) δ 3.49 (s, 3 H), 6.33 (d, J = 9.23 Hz, 1 H), 6.50 (d, J = 9.61 Hz, 1 H), 7.43 (d, J = 9.42 Hz, 1 H), 7.36 (d, J = 9.61 Hz, 1 H); HRMS m/z (ES+) 177.19 $(M + H)^+$ for $C_9H_8N_2O_2$.

1-(2-Hydroxyethyl)-5-methyl-1,5-naphthyridine-2,6(1*H*,5*H*)-dione (8-iv). In a 100 mL round-bottomed flask, **8-iii** (1.000 g, 5.68 mmol) and cesium carbonate (2.034 g, 6.24 mmol) were taken up in DMSO (10 mL) under anitrogen atmosphere to give a yellowish solution. To it was added 2-bromoethanol (0.561 mL, 7.95 mmol), and the resulting reaction mass was heated to 95 °C overnight. Water was added to the reaction mass and extracted using ethyl acetate (5 × 40 mL). The combined organic fractions were washed with water, dried with sodium sulfate, and concentrated to dryness to yield **8-iv** (1.300 g, 104%) as light yellow solid: HRMS m/z (ES+) 221.26 $(M + H)^+$ for $C_{11}H_{12}N_2O_3$.

2-(5-Methyl-2,6-dioxo-5,6-dihydro-1,5-naphthyridin-1(2*H*)-yl)ethylmethanesulfonate (8-v). In 50 mL round-bottomed flask, **8-iv** (400 mg, 1.82 mmol) and TEA (0.759 mL, 5.45 mmol) were taken up in DCM (10 mL) under a nitrogen atmosphere to give a yellowish solution. The resulting reaction mass was cooled to 0 °C and Mesyl-Cl (0.184 mL, 2.36 mmol) was added to it very slowly. Then the reaction mixture was stirred at 0 °C for 45 min. DCM was added to the reaction mass and washed with water (2 × 20 mL). The combined organic fractions were dried over sodium sulfate and concentrated to dryness to yield **8-v** (600 mg, 111%) as a yellow gel: HRMS m/z (ES+) 299.27 $(M + H)^+$ for $C_{12}H_{14}N_2O_5S$.

2-Methyl-5-((1-(2-(5-methyl-2,6-dioxo-5,6-dihydro-1,5-naphthyridin-1(2*H*)-yl)ethyl)piperidin-4-ylamino)methyl)-nicotinonitrile (8). In a 100 mL round-bottomed flask, **8-v** (500 mg, 1.68 mmol), **29e** (386 mg, 1.68 mmol), and sodium carbonate (355 mg, 3.35 mmol) were taken up in DMF (5 mL) to give a yellowish solution under a nitrogen atmosphere that was heated to 70 °C for 1 h. Solvent was evaporated from the reaction mixture. Water was added to the residue and it was extracted using 10% methanol in DCM (3 × 25 mL). The combined organic layers were concentrated to dryness and purified by preparative HPLC to yield **8** (160 mg, 22.07%) as a yellow solid: ^{1}H NMR (400 MHz, DMSO-d_6) δ 1.14−1.27 (m, 2 H), 1.70−1.80 (m, 2 H), 1.96−2.06 (m, 2 H), 2.25−2.36 (m, 2 H), 2.39−2.49 (m, 2 H), 2.65 (s, 3 H), 2.84−2.89 (m, 2 H), 3.62 (s, 3 H), 3.73 (s, 2 H), 4.31 (t, J = 6.78 Hz, 2 H), 6.78 (s, 1 H), 6.76 (s, 1 H), 7.82−8.01 (m, 2 H), 8.15 (d, J = 2.01 Hz, 1 H), 8.66 (d, J = 2.01 Hz, 1 H); HRMS m/z (ES+) 433.235 18 (MH^+) for $C_{24}H_{28}N_6O_2$.

1-(2-(4-((5-Cyano-6-methylpyridin-3-yl)methylamino)-piperidin-1-yl)ethyl)-7-methoxy-2-oxo-1,2-dihydroquinoline-5-carbonitrile (9). In a 100 mL round-bottomed flask, **27i** (500 mg,

dx.doi.org/10.1021/jm500432n | J. Med. Chem. XXXX, XXX, XXX−XXX

1.53 mmol), **32** (416 mg, 1.84 mmol), and sodium carbonate (325 mg, 3.06 mmol) were taken up in DMF (10 mL) to give a yellowish solution under nitrogen atmosphere and heated to 70 °C for 1 h. Solvent was evaporated from the reaction mixture. Water was added to thr residue and it was extracted using 10% methanol in DCM (3 × 25 mL). The combined organic layers were concentrated to dryness and purified by silica gel chromatography to obtain impure product (250 mg) that was repurified by preparative HPLC to give **9** (60.0 mg, 8.58%) as white solid: ^{1}H NMR (400 MHz, DMSO-d_6) δ 1.10−1.33 (m, 2 H), 1.75−1.78 (m, 2 H), 2.02 (t, J = 10.54 Hz, 2 H), 2.15−2.39 (m, 2 H), 2.55 (m, 2H) 2.65 (s, 3 H), 2.89−2.92 (m, 2 H), 3.74 (br s, 2 H), 3.96 (s, 3 H), 4.37 (t, J = 7.03 Hz, 2 H), 6.68 (d, J = 9.54 Hz, 1 H), 7.31 (d, J = 2.01 Hz, 1 H), 7.54 (d, J = 2.51 Hz, 1 H), 7.92 (d, J = 10.04 Hz, 1 H), 8.15 (d, J = 2.01 Hz, 1 H), 8.66 (d, J = 2.01 Hz, 1 H); HRMS m/z (ES+) 457.234 16 (MH$^+$) for $C_{26}H_{28}N_6O_2$.

5-Cyano-*N*-(1-(2-(7-methoxy-2-oxo-1,5-naphthyridin-1(2*H*)-yl)ethyl)piperidin-4-yl)-6-methylnicotinamide (10). In a 50 mL round-bottomed flask **33** (0.161 g, 0.99 mmol) was dissolved in DMF (5 mL) under N_2. To this were added DIPEA (0.520 mL, 2.98 mmol) and HATU (0.754 g, 1.98 mmol), and the mixture was stirred. After 5 min, **27e** (0.300 g, 0.99 mmol) was added. The resulting reaction was at rt for 3 h. DMF was evaporated to dryness, and the residue was diluted with water, extracted with 10% methanol in DCM, and concentrated. Purification was done by preparative HPLC to get pure product **10** (0.200 g, 45.1%): ^{1}H NMR (300 MHz, DMSO-d_6) δ 1.41−1.61 (m, 2 H), 1.80 (d, J = 9.98 Hz, 2 H), 2.05−2.22 (m, 2 H), 2.59 (t, J = 6.59 Hz, 2 H), 2.73 (s, 3 H), 3.01 (d, J = 11.30 Hz, 2 H), 3.77 (dd, J = 7.63, 3.67 Hz, 1 H), 4.00 (s, 3 H), 4.39 (t, J = 6.59 Hz, 2 H), 6.67 (d, J = 9.61 Hz, 1 H), 7.44 (d, J = 2.07 Hz, 1 H), 7.88 (d, J = 9.61 Hz, 1 H), 8.29 (d, J = 2.26 Hz, 1 H), 8.51 (d, J = 7.54 Hz, 1 H), 8.59 (d, J = 2.07 Hz, 1 H), 9.08 (d, J = 2.26 Hz, 1 H); HRMS m/z (ES+) 447.213 98 (MH$^+$) for $C_{24}H_{26}N_6O_3$.

2-Methoxy-5-((1-(2-(7-methoxy-2-oxo-1,5-naphthyridin-1(2*H*)-yl)ethyl)piperidin-4-ylamino)methyl)nicotinonitrile (11). In a 50 mL round-bottomed flask, **27e** (0.050 g, 0.17 mmol) and **34** (0.027 g, 0.17 mmol) were taken in a mixture of ethanol (5 mL) and chloroform (5.00 mL) under N_2. To this was added acetic acid (0.095 μL, 1.65 μmol), and the reaction was stirred at 65 °C. A turbid solution was observed. After 1 h, the reaction was cooled to rt and sodium cyanoborohydride (0.021 g, 0.33 mmol) was added. The resulting reaction was stirred at rt for another 6 h. Reaction solvents were evaporated to dryness and diluted with sat. $NaHCO_3$ solution. The crude mixture was extracted with 5% methanol in DCM and washed with water and brine. The organic layer was separated and concentrated. Purification was done using methanol/DCM as a mobile phase to get pure product **11** (0.045 g, 60.7%): ^{1}H NMR (300 MHz, DMSO-d_6) δ 1.13−1.28 (m, 2 H), 1.77 (d, J = 11.30 Hz, 2 H), 2.04 (t, J = 10.46 Hz, 2 H), 2.16 (br s, 1 H), 2.30 (d, J = 14.51 Hz, 1 H), 2.55 (m, 2H) 2.91 (d, J = 11.68 Hz, 2 H), 3.68 (s, 2 H), 3.98 (s, 6 H), 4.35 (t, J = 6.88 Hz, 2 H), 6.66 (d, J = 9.61 Hz, 1 H), 7.41 (d, J = 2.07 Hz, 1 H), 7.87 (d, J = 9.61 Hz, 1 H), 8.19 (d, J = 2.26 Hz, 1 H), 8.28 (d, J = 2.45 Hz, 1 H), 8.39 (d, J = 2.26 Hz, 1 H); HRMS m/z (ES+) 449.229 26 (MH$^+$) for $C_{24}H_{28}N_6O_3$.

6-((1-(2-(7-Methoxy-2-oxo-1,5-naphthyridin-1(2*H*)-yl)ethyl)-piperidin-4-ylamino)methyl)-3-methylpyrazine-2-carbonitrile (12). In a 25 mL sealed vial, **12a** (95 mg, 0.19 mmol), $ZnCN_2$ (57.2 mg, 0.49 mmol), $Zn(OAc)_2$ (5.72 mg, 0.03 mmol), and Zn (12.75 mg, 0.19 mmol) were added in DMF (5 mL), and then $Pd_2(dba)_3$ (14.28 mg, 0.02 mmol) and dppf (17.29 mg, 0.03 mmol) were added. The mixture was heated to 100 °C for 1 h, filtered through Celite, and washed with 10% MeOH/DCM. The filtrate was concentrated under vacuum, and the crude residue was purified by preparative HPLC to get the required product, which was hygroscopic. The product was dissolved in 1 mL of DCM and cooled to 0 °C, and 1 mL of HCl in diethyl ether was added dropwise. The salt that precipitated was filtered under nitrogen flow to get the 2HCl salt of **12** (23 mg, 23.30%): ^{1}H NMR (300 MHz, DMSO-d_6) δ 2.05−2.20 (m, 2 H), 2.35−2.45 (m, 2 H), 2.77 (s, 3 H), 3.05−3.20 (m, 2 H), 3.25−3.45 (m, 3 H), 3.80−3.88 (m, 2 H), 4.05 (s, 3 H), 4.50−4.55 (m, 2 H), 4.70−4.75 (m, 2 H), 6.75 (d, J = 9.8 Hz, 1 H), 7.70 (s, 1 H), 7.90 (d, J = 9.8 Hz, 1 H), 8.34 (s, 1 H), 9.05 (s, 1 H), 9.95 (br s, 2 H), 11.32 (br s, 1 H); HRMS m/z (ES+) 434.230 91 (MH$^+$) for $C_{23}H_{27}N_7O_2$·2HCl.

5-((1-(2-(6-Methoxy-3-oxopyrido[3,2-*b*]pyrazin-4(3*H*)-yl)-ethyl)piperidin-4-ylamino)methyl)-2-methylnicotinonitrile (13). In a 100 mL round-bottomed flask, 4-(2-(4-aminopiperidin-1-yl)ethyl)-6-methoxypyrido[3,2-*b*]pyrazin-3(4*H*)-one[10] (**27f**) (1.5 g, 4.94 mmol), **32** (1.342 g, 5.93 mmol), and sodium carbonate (0.545 mL, 9.89 mmol) were taken up in DMF (5 mL) to give a brown solution. The resulting reaction mixture was heated to 74 °C for 1 h. The reaction mixture was evaporated, and the residue was taken up in water. The aqueous layer was extracted with DCM (three times). The DCM layer was evaporated and the crude compound was purified by preparative HPLC to give **13** (0.500 g, 20.49%) as a monoacetate salt: ^{1}H NMR (300 MHz, DMSO-d_6) δ 1.26−1.28 (m, 2 H), 1.56−1.57 (m, 2 H), 1.9 (s, 3 H), 2.0−2.1 (m, 2 H), 2.2−2.4 (m,1 H), 2.6−2.7 (m, 1 H), 2.8 (s, 3 H), 2.9−3.0 (m, 2 H), 3.7 (s, 2 H), 4.0 (s, 3 H), 4.2−4.5 (t, 2 H), 6.80 (d, 1 H), 8.0−8.2 (m, 3 H), 8.6 (s, 1 H); HRMS m/z (ES+) 434.230 02 (MH$^+$) for $C_{23}H_{27}N_7O_2$·CH_3COOH.

5-((1-(2-(7-Methoxy-2-oxopyrido[3,2-*b*]pyrazin-1(2*H*)-yl)-ethyl)piperidin-4-ylamino)methyl)-2-methylnicotinonitrile (14). In a 250 mL round-bottomed flask, **27h** (2.000 g, 6.59 mmol), **32** (1.641 g, 7.25 mmol), DIPEA (3.45 mL, 19.78 mmol), and sodium carbonate (1.398 g, 13.19 mmol) were taken up in DMF (25 mL) to give a yellowish solution under nitrogen atmosphere that was heated to 70 °C for 1 h. Solvent was evaporated from the reaction mixture. Water was added to the residue and the mixture was extracted using 10% methanol in DCM (3 × 50 mL). The combined organic layers were concentrated to dryness and purified by silica gel chromatography using 0−35% methanol in DCM and 0.1% ammonia to yield an impure product (700 mg) that was repurified by preparative HPLC to give **14** (0.100 g, 3.50%): ^{1}H NMR (300 MHz, DMSO-d_6) δ 1.07−1.26 (m, 2 H), 1.72−1.75 (m, 2 H), 1.92−2.09 (m, 2 H), 2.22−2.36 (m, 2H) 2.55 (t, J = 6.59 Hz, 2 H), 2.64 (s, 3 H), 2.82−2.96 (m, 2 H), 3.72 (s, 2 H), 4.00 (s, 3 H), 4.34 (t, J = 6.50 Hz, 2 H), 7.51 (d, J = 2.45 Hz, 1 H), 8.14 (d, J = 1.70 Hz, 1 H), 8.25 (s, 1 H), 8.32 (d, J = 2.45 Hz, 1 H), 8.65 (d, J = 1.88 Hz, 1 H); HRMS m/z (ES+) 434.230 32 (MH+) for $C_{23}H_{27}N_7O_2$.

1-(2-((3*S*,4*R*)-4-((5-Cyano-6-methylpyridin-3-yl)-methylamino)-3-fluoropiperidin-1-yl)ethyl)-2-oxo-1,2-dihydroquinoline-7-carbonitrile (15). In a 50 mL round-bottomed flask, **29a** (487 mg, 0.82 mmol) was dissolved in DMF (15 mL), and DIPEA (0.576 mL, 3.30 mmol) was added. The mixture stirred for 5 min, and then **28a**[11] (175 mg, 0.82 mmol) was added. The reaction was heated to 70 °C for 2 h and then brought to rt. Sodium triacetoxyborohydride (524 mg, 2.47 mmol) was added and the mixture was stirred at rt for overnight. The reaction mixture was filtered through a sintered funnel, washed with 20% MeOH in DCM, and concentrated. The crude compound was basified with saturated sodium bicarbonate solution and extracted with 15% MeOH/DCM. The solvent was evaporated under vacuum to yield crude product that was purified by preparative HPLC to give **15** (200 mg, 54.6%): ^{1}H NMR (400 MHz, DMSO-d_6) δ 1.64 (m, 2 H), 2.13 (t, 1 H), 2.40−2.20 (m, 1 H), 2.57 (t, 4 H), 2.87 (s, 3H) 3.14 (m,1H) 2.97 (m, 1 H), 3.80 (s, 2 H), 4.28−4.44 (m, 2 H), 4.65 and 4.78 (s, 1 H), 6.79 (d, J = 9.54 Hz, 1 H), 7.66 (d, J = 8.03 Hz, 1 H), 7.91 (d, J = 8.03 Hz, 1 H), 8.01 (d, J = 9.54 Hz, 1 H), 8.10 (s, 1 H), 8.17 (d, J = 2.01 Hz, 1 H), 8.68 (d, J = 2.01 Hz, 1 H); HRMS m/z (ES+) 445.216 72 (MH$^+$) for $C_{25}H_{25}FN_6O$.

5-(((3*S*,4*R*)-3-Fluoro-1-(2-(7-fluoro-2-oxo-1,5-naphthyridin-1(2*H*)-yl)ethyl)piperidin-4-ylamino)methyl)-2-methylnicotinonitrile (16). In a 100 mL round-bottomed flask, **29a** (520 mg, 2.10 mmol), **28b** (500 mg, 1.75 mmol), and sodium carbonate (370 mg, 3.49 mmol) were taken up in DMF (10 mL) to give a yellowish solution under nitrogen atmosphere that was heated to 70 °C for 1 h. Solvent was evaporated from the reaction mixture. Water was added to the residue and it was extracted using 10% methanol in DCM (3 × 25 mL). The combined organic layers were concentrated to dryness and purified by silica gel chromatography to yield **16** (450 mg, 58.8%) as yellow gel: ^{1}H NMR (400 MHz, DMSO-d_6) δ 1.48−1.63 (m, 1 H), 1.63−1.74 (m, 1 H), 2.10−2.23 (m, 1 H), 2.25−2.44 (m, 2 H), 2.46−2.54 (m, 1 H), 2.63 (t, J = 6.53 Hz, 2 H), 2.70 (s, 3 H), 2.90−3.03 (m,

dx.doi.org/10.1021/jm500432n | J. Med. Chem. XXXX, XXX, XXX−XXX

1 H), 3.11−3.23 (m, 1 H), 3.85 (s, 2 H), 4.26−4.45 (m, 2 H), 4.69−4.81 (2m, 1 H), 6.89 (d, J = 9.54 Hz, 1 H), 8.00 (d, J = 10.04 Hz, 1 H), 8.09 (dd, J = 11.04, 2.01 Hz, 1 H), 8.21 (d, J = 1.51 Hz, 1 H), 8.61 (d, J = 2.51 Hz, 1 H), 8.73 (d, J = 2.01 Hz, 1 H); HRMS m/z (ES+) 439.206 23 (MH^+) for $C_{23}H_{24}F_2N_6O$.

5-(((3*S*,4*R*)-3-Fluoro-1-(2-(7-methoxy-2-oxo-1,5-naphthyridin-1(2*H*)-yl)ethyl)piperidin-4-ylamino)methyl)-2-methylnicotinonitrile (17). In a 500 mL round-bottomed flask, **16** (8.50 g, 19.39 mmol) and sodium methoxide (4.19 g, 77.54 mmol) were taken up in MeOH (150 mL) to give a yellow solution. The resulting reaction mixture was heated to reflux for 2 h. Solvent was evaporated from the reaction mixture, and water was added to the residue. This was extracted using 10% methanol in DCM (3 × 200 mL), and the combined organic layers were concentrated and purified by silica gel chromatography using 0−10% methanol in DCM to yield **17** (5.5 g) as off white solid, which was low-melting and hygroscopic. Therefore, the free base was dissolved in DCM (60 mL), and HCl in ether (85 mL) was added to it. The precipitated solid was stirred at rt for 2 h and filtered. The filtered solid was further triturated with methanol/acetonitrile, filtered, and dried to give the HCl salt of **17** (6.50 g, 64.1%) as pale yellow solid: ^{1}H NMR (300 MHz, DMSO-d_6) δ 2.18−2.47 (m, 2 H), 2.72 (s, 3 H), 3.23−3.75 (m, 7 H), 4.07 (s, 3 H), 4.26−4.46 (m, 2 H), 4.63−4.86 (m, 2 H), 5.50−5.66 (d, J = 45 Hz 1H), 6.73 (d, J = 9.80 Hz, 1 H), 7.75 (s, 1 H), 7.95 (d, J = 9.80 Hz, 1 H), 8.34 (d, J = 2.07 Hz, 1 H), 8.57 (d, J = 2.07 Hz, 1 H), 8.95 (d, J = 2.07 Hz, 1 H), 10.22−10.33 (2 br s, 2 H), 11.25 (br s, 1 H); HRMS m/z (ES+) 451.225 43 (MH^+) for $C_{24}H_{27}FN_6O_2{\cdot}2HCl$.

5-(((3*S*,4*R*)-3-Methoxy-1-(2-(7-methoxy-2-oxo-1,5-naphthyridin-1(2*H*)-yl)ethyl)piperidin-4-ylamino)methyl)-2-methylnicotinonitrile (18). In a 50 mL round-bottomed flask, **18b** (150 mg, 0.45 mmol) was dissolved in DMF (5 mL), sodium carbonate (143 mg, 1.35 mmol) was added, and the mixture was stirred for 2 min. Then **32** (102 mg, 0.45 mmol) was added to the reaction and heated to 70 °C for 2 h. The reaction mixture was concentrated under vacuum, and the residue was basified with saturated $NaHCO_3$ solution, concentrated under vacuum, and purified by preparative HPLC to give **18** (30.0 mg, 12.42%) as a gum: ^{1}H NMR (300 MHz, DMSO-d_6) δ 1.35−1.52 (m, 1 H), 1.58−1.74 (m, 1 H), 1.97−2.11 (m, 1 H), 2.20−2.44 (m, 2 H), 2.54−2.61 (m, 2 H), 2.61−2.85 (m, 6 H), 3.17 (s, 3 H), 3.25−3.32 (m, 1 H), 3.74 (d, J = 4.33 Hz, 2 H), 3.98 (s, 3 H), 4.27−4.44 (m, 2 H), 6.66 (d, J = 9.61 Hz, 1 H), 7.43 (s, 1 H), 7.86 (d, J = 9.80 Hz, 1 H), 8.17 (s, 1 H), 8.27 (d, J = 2.07 Hz, 1 H), 8.67 (s, 1 H); HRMS m/z (ES+) 463.245 32 (MH^+) for $C_{25}H_{30}N_6O_3$.

6-(((3*S*,4*R*)-3-Fluoro-1-(2-(7-fluoro-2-oxo-1,5-naphthyridin-1(2*H*)-yl)ethyl)piperidin-4-ylamino)methyl)-2*H*-pyrido[3,2-*b*][1,4]oxazin-3(4*H*)-one (19). In a 250 mL round-bottomed flask, **28b** (7.86 g, 27.47 mmol), **29b** (7.00 g, 24.97 mmol), and sodium carbonate (5.29 g, 49.95 mmol) were taken up in DMF (50 mL) to give a yellowish solution under nitrogen atmosphere that was heated to 70 °C for 1 h. Solvent was evaporated from the reaction mixture. Water was added to the residue and it was extracted using 10% methanol in DCM (5 × 75 mL). The combined organic layers were concentrated to dryness and purified by silica gel column using 0−12% methanol in DCM to yield **19** (5.40 g, 46.0%) as a white solid: ^{1}H NMR (300 MHz, DMSO-d_6) δ 1.44−1.68 (m, 2 H), 2.2−2.39 (m, 3 H), 2.57 (t, J = 6.59 Hz, 2 H), 2.84−2.97 (m, 1 H), 3.06−3.20 (m, 1 H), 3.60−3.82 (m, 2 H), 4.14−4.43 (m, 2 H), 4.61 (s, 3 H), 4.63−4.79 (d, J = 45 Hz, 1 H), 6.83 (d, J = 9.80 Hz, 1 H), 7.02 (d, J = 8.10 Hz, 1 H), 7.30 (d, J = 7.91 Hz, 1 H), 7.95 (d, J = 9.80 Hz, 1 H), 8.04 (dd, J = 11.21, 2.17 Hz, 1 H), 8.56 (d, J = 2.26 Hz, 1 H), 11.20 (s, 1 H); HRMS m/z (ES+) 471.196 74 (MH^+) for $C_{23}H_{24}F_2N_6O_3$.

6-(((3*R*,4*S*)-3-Fluoro-1-(2-(7-fluoro-2-oxo-1,5-naphthyridin-1(2*H*)-yl)ethyl)piperidin-4-ylamino)methyl)-2*H*-pyrido[3,2-*b*][1,4]oxazin-3(4*H*)-one (20). In a 250 mL round-bottomed flask, **29c** (3.50 g, 12.49 mmol) was dissolved in DMF (50 mL) and Na_2CO_3 (3.97 g, 37.46 mmol) was added. The mixture stirred for 2 min, **28b** (4.29 g, 14.98 mmol) was added, and the reaction was heated to 70 °C for 2 h. The reaction mixture was concentrated under vacuum, and the residue was basified with sat. $NaHCO_3$ solution, concentrated under vacuum, and purified by preparative HPLC to give **20** (2.90 g, 49.4%): ^{1}H NMR (300 MHz, DMSO) δ 1.41−1.70 (m, 2 H), 1.93−2.19 (m, 3 H), 2.19−2.42 (m, 1 H), 2.57 (t, J = 6.69 Hz, 3 H), 2.90 (d, J = 11.30 Hz, 1 H), 3.02−3.22 (m, 1 H), 3.71 (d, J = 3.39 Hz, 2 H), 4.30 (tq, J = 13.10, 6.77 Hz, 2 H), 4.60 (s, 1 H), 4.64−4.79 (d, J = 45 Hz 1 H), 6.83 (d, J = 9.61 Hz, 1 H), 7.02 (d, J = 8.10 Hz, 1 H), 7.30 (d, J = 8.10 Hz, 1 H), 7.95 (d, J = 9.80 Hz, 1 H), 7.99−8.11 (m, 1 H), 8.56 (d, J = 2.07 Hz, 1 H), 11.19 (s, 1 H); HRMS m/z (ES+) 471.196 93 (MH^+) for $C_{23}H_{24}F_2N_6O_3$.

6-(((3*S*,4*R*)-3-Fluoro-1-(2-(7-methoxy-2-oxo-1,5-naphthyridin-1(2*H*)-yl)ethyl)piperidin-4-ylamino)methyl)-2*H*-pyrido[3,2-*b*][1,4]oxazin-3(4*H*)-one (21). In a 50 mL round-bottomed flask, **28c** (350 mg, 1.17 mmol), **29b** (803 mg, 1.29 mmol), DIPEA (0.615 mL, 3.52 mmol), and sodium carbonate (249 mg, 2.35 mmol) were taken up in DMF (5 mL) to give a yellowish solution under nitrogen atmosphere that was heated to 70 °C for 1 h. Solvent was evaporated from the reaction mixture. Water was added to the residue and extracted using 10% methanol in DCM (3 × 25 mL). The combined organic layers were concentrated to dryness and purified by preparative HPLC to yield **21** (120 mg, 21.20%) as white solid: ^{1}H NMR (300 MHz, DMSO-d_6) δ 1.46−1.74 (m, 2 H), 2.16 (t, J = 10.27 Hz, 1 H), 2.24−2.45 (m, 2 H), 2.59 (t, J = 6.88 Hz, 3 H), 2.86−2.98 (m, 1 H), 3.08−3.17 (m, 1 H), 3.73 (s, 2 H), 3.99 (s, 3 H), 4.27−4.44 (m, 2 H), 4.61 (s, 2 H), 4.65−4.82 (2m, 1 H), 6.66 (d, J = 9.61 Hz, 1 H), 7.02 (d, J = 8.10 Hz, 1 H), 7.30 (d, J = 7.91 Hz, 1 H), 7.42 (d, J = 2.26 Hz, 1 H), 7.87 (d, J = 9.61 Hz, 1 H), 8.28 (d, J = 2.26 Hz, 1 H), 11.15 (br s, 1 H); HRMS m/z (ES+) 483.215 93 (MH^+) for $C_{24}H_{27}FN_6O_4$.

6-(((3*R*,4*S*)-3-Fluoro-1-(2-(7-methoxy-2-oxo-1,5-naphthyridin-1(2*H*)-yl)ethyl)piperidin-4-ylamino)methyl)-2*H*-pyrido[3,2-*b*][1,4]oxazin-3(4*H*)-one (22). In a 100 mL round-bottomed flask, **22a** (1.5 g, 3.19 mmol) was dissolved in MeOH (30 mL), and sodium methoxide (0.689 g, 12.75 mmol) was added. The mixture was heated to 80 °C overnight. The solvent was evaporated under vacuum, the residue was basified with saturated $NaHCO_3$ solution and extracted with 10% MEOH/DCM, and the solvent was evaporated to get the crude compound, which was purified by preparative HPLC to give **22** (1.2 g, 78%): ^{1}H NMR (300 MHz, DMSO-d_6) δ 1.46−1.76 (m, 2 H), 1.96−2.22 (m, 2 H), 2.22−2.45 (m, 1 H), 2.57 (t, J = 6.78 Hz, 3 H), 2.93 (d, J = 11.30 Hz, 1 H), 3.15 (br s, 1 H), 3.72 (s, 2 H), 3.92−4.09 (m, 3 H), 4.35 (t, J = 6.22 Hz, 2 H), 4.60 (s, 2 H), 4.63−4.88 (d, J = 51 Hz, 1 H), 6.66 (d, J = 9.61 Hz, 1 H), 7.02 (d, J = 8.10 Hz, 1 H), 7.30 (d, J = 8.10 Hz, 1 H), 7.42 (s, 1 H), 7.87 (d, J = 9.61 Hz, 1 H), 8.28 (s, 1 H), 11.19 (s, 1 H); HRMS m/z (ES+) 483.216 40 (MH^+) for $C_{24}H_{27}FN_6O_4$.

6-(((3*S*,4*R*)-3-Methoxy-1-(2-(7-methoxy-2-oxo-1,5-naphthyridin-1(2*H*)-yl)ethyl)piperidin-4-ylamino)methyl)-2*H*-pyrido-[3,2-*b*][1,4]oxazin-3(4*H*)-one (23). In a 250 mL round-bottomed flask, **23c** (2.300 g, 4.77 mmol) and sodium methoxide (1.288 g, 23.83 mmol) were taken up in MeOH (50 mL) to give a white solution under nitrogen atmosphere and heated to 70 °C for 2 h. The solvent was evaporated from the reaction mixture. Water was added to the residue and extracted using 10% methanol in DCM (3 × 100 mL). The combined organic layers were concentrated to dryness and purified by silica gel chromatography using 0−10% methanol in DCM and 0.1% ammonia to yield **23** (0.350 g, 14.85%) as off white solid: ^{1}H NMR (300 MHz, DMSO) δ 1.73 (br s, 2 H), 1.99−2.20 (m, 2 H), 2.51−2.71 (m, 2 H), 2.99 (br s, 1 H), 3.09−3.23 (m, 4 H), 3.62 (br s, 1H), 3.94 (s, 3 H), 3.95−4.10 (m, 3 H), 4.21−4.47 (m, 2 H), 4.63 (s, 2 H), 6.61 (d, J = 9.61 Hz, 1 H), 7.06 (d, J = 7.91 Hz, 1 H), 7.30−7.47 (m, 2 H), 7.83 (d, J = 9.61 Hz, 1 H), 8.24 (d, J = 2.07 Hz, 1H), 8.75 (br s, 1H), 11.30 (s, 1H); HRMS m/z (ES+) 495.230 61 (MH^+) for $C_{25}H_{30}N_6O_5$.

■ ASSOCIATED CONTENT

Ⓢ Supporting Information

Sythetic schemes and procedures for intermediates; primary sequence alignment of Mtb GyrA and Sau GyrA; Overlay of secondary structures of Mtb GyrA model and Sau GyrA; comparison of active site residues of Mtb GyrA model and Sau GyrA crystal structure; docked poses of compounds **1a**, **2a**, and

dx.doi.org/10.1021/jm500432n | J. Med. Chem. XXXX, XXX, XXX−XXX

19; comparison of the binding mode of FQ and NBTIs in the Sau DNA gyrase crystal structure; assay procedures for log *D* and hERG measurement. This material is available free of charge via the Internet at http://pubs.acs.org.

AUTHOR INFORMATION

Corresponding Author

*Phone: +91 80 23621212, Ext. 6292. Fax: +91 80 23621214. E-mail: shahul.mehar@astrazeneca.com; shahulmehar@yahoo.com.

Present Addresses

[⊥]Medicines for Malaria Venture (MMV), Geneva, Switzerland. [#]Swedish Institute for Communicable Disease Control, S-171 82 Solna, Sweden.

Notes

The authors declare no competing financial interest.

ACKNOWLEDGMENTS

We sincerely thank CMG Bangalore, AZ Global DMPK, Safety, Biosciences (AZ, Boston, MA), and Discovery Sciences (AZ, Alderly Park, UK) for technical support in various assays. We acknowledge Sandeep Ghorpade, Manoranjan Panda, and Pravin Shirude for scientific discussions. We also thank V. Balasubramanian, R. Tommasi, and Tanjore Balganesh for their constant inspiration, support, and encouragement.

ABBREVIATIONS USED

TB, tuberculosis; FQ, fluoroquinolone; Mtb, *Mycobacterium tuberculosis*; Msm, *Mycobacterium smegmatis*; MIC, minimum inhibitory concentration; HB, H-bond; SAR, structure−activity relationship; SPR, structure−property relationship; AUC, area under the curve; cfu, colony forming units; rt, room temperature; DME, 1,2-dimethoxyethane; THF, tetrahydrofuran; DMF, *N*,*N*-dimethylformamide; ABT, aminobenzotriazole; BSL-3, biosafety level 3 laboratory.

REFERENCES

(1) World Health Organization. Global tuberculosis control. WHO 2012 report (http://www.who.int/mediacentre/news/releases/2011/tb_20111011/en/index.html); WHO: Geneva, 2012.

(2) World Health Organization. Multidrug and extensively drug-resistant TB (M/XDR-TB); WHO 2010 Global report on surveillance and response; WHO: Geneva, 2010.

(3) Cole, S. T.; Brosch, R.; Parkhill, J.; Garnier, T.; Churcher1, C.; Harris, D.; Gordon, S. V.; Eiglmeier, K.; Gas, S.; Barry, C. E., III; Tekaia, F.; Badcock, K.; Basham, D.; Brown, D.; Chillingworth, T.; Connor, R.; Davies, R.; Devlin, K.; Feltwell, T.; Gentles, S.; Hamlin, N.; Holroyd, S.; Hornsby, T.; Jagels, K.; Krogh, A.; McLean, J.; Moule, S.; Murphy, L.; Oliver, K.; Osborne, J.; Quail, M. A.; Rajandream, M.-A.; Rogers, J.; Rutter, S.; Seeger, K.; Skelton, J.; Squares, R.; Squares, S.; Sulston, J. E.; Taylor, K.; Whitehead, S.; Barrell, B. G. Deciphering the biology of *Mycobacterium tuberculosis* from the complete genome sequence. *Nature* **1998**, *393*, 537−544.

(4) Sharma, U. Current possibilities and unresolved issues of drug target validation in *Mycobacterium tuberculosis*. *Expert Opin. Drug Discovery* **2011**, *6*, 1171−1186.

(5) (a) Burman, W. J.; Goldberg, S.; Johnson, J. L.; Muzanye, G.; Engle, M.; Mosher, A. W.; Choudhari, S.; Daley, C. L.; Munsiff, S. S.; Zhao, Z.; Vernon, A.; Chaisson, R. E. Moxifloxacin versus ethambutol in the first 2 months of treatment for pulmonary tuberculosis. *Am. J. Respir. Crit. Care Med.* **2006**, *174*, 331−338. (b) Conde, M. B.; Efron, A.; Loredo, C.; De Souza, G. R.; Graca, N. P.; Cezar, M. C.; Ram, M.; Chaudhary, M. A.; Bishai, W. R.; Kritski, A. L.; Chaisson, R. E. Moxifloxacin in the initial therapy of tuberculosis: A randomized, phase 2 trial. *Lancet* **2009**, *373*, 1183−1189. (c) Diacon, A. H.; Dawson, R.; von Groote-Bidlingmaler, F.; Symons, G.; Venter, A.; Donald, P. R.; van Niekerk, C.; Everitt, D.; Winter, H.; Becker, P.; Mendel, C. M.; Spigelman, M. K. 14 day bactericidal activity of PA-824, bedaquiline, pyrazinamide, and moxifloxacin combinations: A randomized trial. *Lancet* **2012**, *380*, 986−993. (d) Duong, D. A.; Nguyen, T. H.; Nguyen, T. N.; Dai, V. H.; Dang, T. M.; Vo, S. K.; Do, D. A.; Nguyen, V. V.; Nguyen, H. D.; Dinh, N. S.; Farrar, J.; Caws, M. Beijing genotype of *Mycobacterium tuberculosis* is significantly associated with high-level fluoroquinolone resistance in Vietnam. *Antimicrob. Agents Chemother.* **2009**, *53*, 4835−4839.

(6) Drlica, K.; Malik, M.; Kerns, R. J.; Zhao, X. Quinolone-mediated bacterial death. *Antimicrob. Agents Chemother.* **2008**, *52*, 385−392.

(7) (a) Bisacchi, G S.; Dumas, J. Recent advances in the inhibition of bacterial type II topoisomerases. In *Annual Reports in Medicinal Chemistry*; Macor, J. E., Ed.; Academic Press: Burlington, MA, 2009; Vol. *44*, pp 379−396. (b) Shirude, P. S.; Hameed, S. Non-fluoroquinolone-based inhibitorsof mycobacterial type II topoisomerase as potential therapeutic agentsfor TB. In *Annual Reports in Medicinal Chemistry*; Desai, M. C., Ed.; Academic Press: Burlington, MA, 2012; Vol. *47*, pp 319−330.

(8) (a) Bax, B. D.; Chan, P. F.; Eggleston, D. S.; Fosberry, A.; Gentry, D. R.; Gorrec, F.; Giordano, I.; Hann, M. M.; Hennessy, A.; Hibbs, M.; Huang, J.; Jones, E.; Jones, J.; Brown, K. K.; Lewis, C. J.; May, E. W.; Saunders, M. R.; Singh, O.; Spitzfaden, C. E.; Shen, C.; Shillings, A.; Theobald, A. J.; Wohlkonig, A.; Pearson, N. D.; Gwynn, M. N. Type IIA topoisomerase inhibition by a new class of antibacterial agents. *Nature* **2010**, *466*, 935−940. (b) Tretter, E. M.; Schoeffler, A. J.; Weisfild, S. R.; Berger, J. M. Crystal structure of the DNA gyrase GyrA N-terminal domain from *Mycobacterium tuberculosis*. *Proteins* **2010**, *78*, 492−495.

(9) (a) Breault, G.; Eyermann, C. J.; Geng, B.; Morningstar, M.; Reck, F. Preparation of quinolinones and analogs for the treatment of multi-drug resistant bacterial infections. WO2006134378, 2006. (b) Janelle,C. P.; Mark, C.; Geng, B.; Aydon, G. A.; Reck, F. Preparation of 2-quinolinone and 2-quinoxalinone derivatives as antibacterial agents. WO2008071961, 2008. (c) Breault, G.; Vincent, G.; Reck, F. Preparation of naphthyridines as bactericides for treating bacterial infections. WO2008071964, 2008. (d) Geng, B.; Morningstar, M.; Reck, F. Preparation of piperidines for the treatment of bacterial infections. WO2008071981, 2008.

(10) Reck, F.; Alm, R.; Brassil, P.; Newman, J.; DeJonge, B.; Eyermann, C. J.; Breault, G.; Breen, J.; Comita-Prevoir, J.; Cronin, M.; Davis, H.; Ehmann, D.; Galullo, V.; Geng, B.; Grebe, T.; Morningstar, M.; Walker, P.; Hayter, B.; Fisher, S. Novel N-linked aminopiperidine inhibitors of bacterial topoisomerase type II: Broad-spectrum antibacterial agents with reduced hERG activity. *J. Med. Chem.* **2011**, *54*, 7834−7847.

(11) Reck, F.; Alm, R.; Brassil, P.; Newman, J.; Ciaccio, P.; McNulty, J.; Barthlow, H.; Goteti, K.; Breen, J.; Comita-Prevoir, J.; Cronin, M.; Ehmann, D.; Geng, B.; Godfrey, A.; Fisher, S. Novel N-Linked aminopiperidine inhibitors of bacterial topoisomerase type II with reduced pKa: Antibacterial agents with an improved safety profile. *J. Med. Chem.* **2012**, *55*, 6916−6933.

(12) (a) Alemparte-Gallardo, C.; Ballell-Pages, L.; Barros-Aguirre, D.; Cacho-Izquierdo, M.; Castro-Pichel, J.; Fiandor Roman, J. M.; Hennessy, A. J.; Pearson, N. D.; Remuinan-Blanco, J. M. Naphthyridin-2(1*H*)-one compounds as antibacterial agents and their preparation, pharmaceutical compositions and use in the treatment of tuberculosis. WO 2009090222, 2009. (b) Alemparte-Gallardo, C.; Barfoot, C.; Barros-Aguirre, D.; Cacho-Izquierdo, M.; Fiandor Roman, J. M.; Hennessy, A. J.; Pearson, N. D.; Remuinan-Blanco, M. J. Preparation of tricyclic nitrogen containing compounds as antibacterials. WO2009141398, 2009. (c) Alemparte-Gallardo, C.; Barros-Aguirre, D.; Cacho-Izquierdo, M.; Fiandor-Roman, J. M.; Lavandera Diaz, J. L.; Remuinan-Blanco, M. J. Naphthyridin-2(1*H*)-one compounds as antibacterials and their preparation and use for the treatment of bacterial infections. WO2010081874, 2010. (d) Miles, T. J.; Hennessy, A. J.; Bax, B.; Brooks, G.; Brown, B. S.; Brown, P.;

Cailleau, N.; Chen, D.; Dabbs, S.; Davies, T. D.; Esken, J. M.; Giordano, L.; Hoover, J. L.; Huang, J.; Jones, G. E.; Sukmar, S. K. K.; Spitzfaden, C.; Markwell, R. E.; Mlingthorn, E. A.; Rittenhouse, S.; Gwynn, M. N.; Pearson, N. D. Novel hydroxyl tricyclics (e.g., GSK966587) as potent inhibitors of bacterial type IIA topoisomerases. *Bioorg. Med. Chem. Lett.* **2013**, *23*, 5437−5441.

(13) (a) Barrows, D. Recent advances in TB drug development. 40th IUATLD Meeting, Cancun, Mexico, 2009. (b) Presentations, 2009. http://www.newtbdrugs.org/eventfiles/p4/Novel%20Mtb%20DNA%20Gyrase%20inhibitors_The%20Union_40th.pdf.

(14) Eric, A. V.; Hao, Y.; Susan, V. D.; Stacie, A. C.; Hayao, M.; Ilaria, G.; Alan, J. H.; Richard, M. G.; Jeffery, L. W. Target-directed synthesis of antibacterial drug candidate GSK966587. *Org. Lett.* **2010**, *12*, 3422−3425.

(15) Ballell, L.; Barros, D.; Brooks, G.; Castro, P. J.; Dabbs, S.; Daines, R. A.; Davies, D. T.; Fiandor, R. J. M.; Giardano, I.; Hennessy, A. J.; Hoffman, J. B.; Jones, G. E.; Miles, T. J.; Peason, N. D.; Pendrak, I.; Remuinan, B. M. J.; Rossi, J. A.; Zhang, L. L. Derivatives and analog of *N*-ethylquinolones and *N*-ethylazaquinolones as antibacterial agents and their preparation. WO2008009700, 2008.

(16) (a) Brooks, G.; Dabbs, S.; Davies, T. D.; Hennessy, A. J.; Jones, G. E.; Markwell, R. E.; Miles, T. J.; Owston, N. A.; Pearson, N. D.; Peng, T. W. The design of efficient and selective routes to pyridyl analogues of 3-oxo-3,4-dihydro-2*H*-1,4-(benzothiazine or benzoxazine)-6-carbaldehydes. *Tetrahedron Lett.* **2010**, *51*, 5035−5037. (b) Hameed, P. S.; Shanbhag, G.; Shinde, V.; Chinnapattu, M.; Manjrekar, P.; Puttur, J.; Patil, V.; Ugarkar, B. Short and efficient synthesis of oxazinone and thiazinone containing bicyclic heteroaromatic aldehydes. *Syn.com.* **2013**, *43*, 3315−3321.

(17) Shandil, R. K.; Jayaram, R.; Kaur, P.; Gaonkar, S.; Suresh, B. L.; Mahesh, B. N.; Jayashree, R.; Nandi, V.; Bharath, S.; Balasubramanian, V. Moxifloxacin, ofloxacin, sparfloxacin, and ciprofloxacin against *Mycobacterium tuberculosis*: Evaluation of in vitro and pharmacodynamic indices that best predict in vivo efficacy. *Antimicrob. Agents Chemother.* **2007**, *51*, 576−82.

(18) (a) Brvar, M.1.; Perdih, A.; Renko, M.; Anderluh, G.; Turk, D.; Solmajer, T. Structure-based discovery of substituted 4,5′-bithiazoles as novel DNA gyrase inhibitors. *J. Med. Chem.* **2012**, *55*, 6413−6426. (b) Shirude, P. S.; Madhavapeddi, P.; Tucker, J. A.; Murugan, K.; Patil, V.; Basavarajappa, H.; Raichurkar, A. V.; Humnabadkar, V.; Hussein, S.; Sharma, S.; Ramya, V. K.; Narayan, C. B.; Balganesh, T. S.; Sambandamurthy, V. K. Aminopyrazinamides. Novel and specific GyrB inhibitors that kill replicating and nonreplicating *Mycobacterium tuberculosis*. *ACS Chem. Biol.* **2013**, *8*, 519−523. (c) Kale, M. G.; Raichurkar, A.; Hameed, S. P.; Waterson, D.; McKinney, D.; Manjunatha, M. R.; Kranthi, U.; Koushik, K.; Jena, L.; Shinde, V.; Rudrapatna, S.; Barde, S.; Humnabadkar, V.; Madhavapeddi, P.; Basavarajappa, H.; Ghosh, A.; Ramya, V. K.; Guptha, S.; Sharma, S.; Vachaspati, P.; Mahesh Kumar, K. N.; Giridhar, J.; Reddy, J.; Panduga, V.; Ganguly, S.; Ahuja, V.; Gaonkar, S.; Naveen Kumar, C. N.; Ogg, D.; Tucker, J. A.; Bori-ack-Sjodin, A. P.; de Sousa, S. M.; Sambandamurthy, V. K.; Ghorpade, S. R. Thiazolopyridine ureas as novel antitubercular agents acting through inhibition of DNA gyrase B. *J. Med. Chem.* **2013**, *56*, 8834−8848. (d) Hameed, S. P.; Solapure, S.; Mukherjee, K.; Nandi, V.; Waterson, D.; Shandil, R.; Balganesh, M.; Sambandamurthy, V. K.; Raichurkar, A.; Deshpande, A.; Ghosh, A.; Awasthy, D.; Shanbhag, G.; Sheikh, G.; McMiken, H.; Puttur, P.; Reddy, J.; Werngren, J.; Read, J.; Kumar, M.; Ramaiah, M.; Chinnapattu1, M.; Madhavapeddi, P.; Manjrekar, P.; Basu, R.; Gaonkar, S.; Sharma, S.; Hoffner, S.; Humnabadkar, V.; Subbulakshmi, V.; Panduga, V. Optimization of pyrrolamides as mycobacterial GyrB ATPase inhibitors: Structure−activity relationship and in vivo efficacy in a mouse model of tuberculosis. *Antimicrob. Agents Chemother.* **2013**, *58*, 6−70. (e) Kale, R. R.; Kale, M. G.; Waterson, D.; Raichurkar, A.; Hameed, S. P.; Manjunatha, M. R.; Kishore Reddy, B. K.; Malolanarasimhan, K.; Shinde, V.; Koushik, K.; Jena, L. K.; Menasinakai, S.; Humnabadkar, V.; Madhavapeddi, P.; Basavarajappa, H.; Sharma, S.; Nandishaiah, R.; Mahesh Kumar, K. N.; Ganguly, S.; Ahuja, V.; Gaonkar, S.; Naveen Kumar, C. N.; Ogg, D.; Boriack-Sjodin, P. A.; Sambandamurthy, V. K.; de Sousa, S. M.; Ghorpade, S. R. Thiazolopyridone ureas as DNA gyrase B inhibitors: Optimization of antitubercular activity and efficacy. *Bioorg. Med. Chem. Lett.* **2014**, *24*, 870−879.

(19) (a) *ROCS 3.2.0.4*; OpenEye Scientific Software, Santa Fe, NM. http://www.eyesopen.com. (b) Hawkins, P. C. D.; Skillman, A. G.; Nicholls, A. Comparison of shape-matching and docking as virtual screening tools. *J. Med. Chem.* **2007**, *50*, 74−82.

(20) *Molecular operating environment (MOE), 2013.08*; Chemical Computing Group Inc., 1010 Sherbooke St. West, Suite #910, Montreal, QC, Canada H3A 2R7, 2013.

(21) (a) *FRED 2.0*; OpenEye scientific software, Santa Fe, NM. http://www.eyesopen.com. (b) McGann, M. FRED pose prediction and virtual screening accuracy. *J. Chem. Inf. Model* **2011**, *51*, 578−596.

(22) McGrath, M.; Gey van Pittius, N. C.; Sirgel, F. A.; Van Helden, P. D.; Warren, R. M. Moxifloxacin retains anti-mycobacterial activity in the presence of gyrA mutations. *Antimicrob. Agents Chemother.* **2014**, *58*, 2912−2915.

(23) Jayaram, R.; Gaonkar, S.; Kaur, P.; Suresh, B. L.; Mahesh, B. N.; Jayashree, R.; Nandi, V.; Bharat, S.; Shandil, R. K.; Kantharaj, E.; Balasubramanian, V. Pharmacokinetics−pharmacodynamics of rifampin in an aerosol infection model of tuberculosis. *Antimicrob. Agents Chemother.* **2003**, *47*, 2118−2124.

(24) Huitric, E.; Verhasselt, P.; Andries, K.; Hoffner, S. E. In vitro antimycobacterial spectrum of a diarylquinoline ATP synthase inhibitor. *Antimicrob. Agents Chemother.* **2007**, *51*, 4202−4204.